Mobility of antimony in contrasting surface environments of a mine site: influence of redox conditions and microbial communities

Jesús Daniel Peco, Hugues Thouin, José María Esbrí, Héctor Ricardo Campos-Rodríguez, Eva Maria García-Noguero, Dominique Breeze, Jaime Villena, Eric Gloaguen, Pablo Leon Higueras, Fabienne Battaglia-Brunet

Mobility of antimony in contrasting surface environments of a mine site – Influence of redox conditions and microbial communities

Jesús Daniel Peco Palacios[1,5], Hugues Thouin[2], José María Esbrí[3], Héctor R. Campos-Rodríguez [4], Eva Maria García-Noguero [1], Dominique Breeze[2], Jaime Villena[5], Eric Gloaguen[4], Pablo Leon Higueras [1], Fabienne Battaglia-Brunet[4*]

1. Instituto de Geología Aplicada, Escuela Universitaria Politécnica de Almadén, Universidad de Castilla-La Mancha, Plaza Manuel Meca, 13400, Almadén, Ciudad Real, Spain
2. BRGM, 3 av. Claude Guillemin, 45060 Orléans, France
3. Departamento de Mineralogía y Petrología, Facultad de Ciencias Geológicas, Universidad. Complutense, 28040 Madrid, Spain
4. Université d'Orléans, CNRS, BRGM, ISTO, UMR 7327, 45071 Orléans, France.
5. Escuela Técnica Superior de Ingenieros Agrónomos de Ciudad Real, Universidad de Castilla-La Mancha, Ronda de Calatrava 7, 13071 Ciudad Real, Spain

*Corresponding author. Email address: f.battaglia@brgm.fr

Abstract

Microbial processes can influence the complex geochemical behaviour of the toxic metalloid antimony (Sb) in mining environments. The present study is aimed to evaluate the influence of microbial communities on the mobility of Sb from solid phases to water in different compartments and redox conditions of a mining site in southwest (SW) Spain. Samples of surface materials presenting high Sb concentrations, from two weathered mining waste dumps and an aquatic sediment were incubated in slurries comparing oxic and anoxic conditions. The initial microbial communities of the three materials strongly differed. Incubations induced an increase of microbial biomass and an evolution of the microbial communities' structures and compositions, which diverged in different redox conditions. The presence of active bacteria always influenced the mobility of Sb, except in the neutral pH waste incubated in oxic

conditions. The effect of active microbial activities in oxic conditions was dependent on the material: Sb oxic release was biologically amplified with the acidic waste, but attenuated with the sediment. Different bacterial genera involved in Sb, Fe, and S oxidation or reduction were present and/or grew during incubation of each material. The results highlighted the wide diversity of microbial communities and metabolisms at the small geographic scale of a mining site and their strong implication in Sb mobility.

Key words: antimony, microbial communities, redox conditions, incubations, mine waste, aquatic sediment

1. Introduction

Antimony (Sb) is a strategic element with a large range of applications. It is involved as a flame retardant in the composition of plastics, coatings and electronics, but also utilised in manufacturing batteries, ammunitions, glasses, semiconductors, diodes, infrared detectors, paints, rubbers, and Hall-effect devices (Krachler et al. 2001; Dupont et al. 2016). The current order of magnitude of annual Sb production is 150,000 tons (USGS 2021). Antimony is mainly extracted from stibnite (Sb_2S_3) mines, but also from Sb oxides and, as a secondary product, from Pb, Au, Ag, Cu, Ni or Zn ores (Anderson 2012; Dupont et al. 2016; Herath et al. 2017). This element, although necessary for the elaboration of many manufactured products, presents health and environmental issues. Acute and chronic toxicity of Sb have been reported (Sundar and Chakravarty 2010). Results from recent studies indicate that Sb might be genotoxic (El Shanawany et al. 2017), and Sb trioxide has been recognised as a potential carcinogen (Schildroth et al. 2021).

Antimony concentration in water compartments of mining environments, i.e. porewater, groundwater and surface water, ranges from a few μg L^{-1} to more than 10 μg L^{-1} (Ashley et al. 2003; Casiot et al. 2007; Filella et al. 2009; Fawcett et al. 2015; Cidu et al. 2018; Radková et al. 2020). In most cases, Sb(V) is the main Sb chemical species detected in solution (Casiot

et al. 2007; Fawcett et al. 2015; Cidu et al. 2015), suggesting that the oxidation state is a major driver of Sb mobility. From a geochemical point of view, environmental behaviour of Sb depends on its speciation, redox conditions, pH, and the presence of major and trace elements, as Sb can be integrated in a large range of secondary minerals (Roper et al. 2012; Herath et al. 2017). Climatic conditions and mineralogy influence the biogeochemical Sb transfer and soil enzymatic parameters in mining environments (Gallego et al. 2021; Esbrí et al. 2022). Meanwhile, the microbial communities naturally present in most environments may influence Sb mobility through several indirect or direct processes.

Aerobic dissolution of Sb sulphides by S- and Fe-oxidising bacteria classically involved in acid mine drainage generation has been shown to produce high Sb concentrations in acidic liquors (Torma and Gabra 1977; Hafeez et al. 2017). Conversely, in anoxic zones, where microbial sulphate reduction occurs, Sb might be chemically reduced by dissolved sulphide (Polack et al. 2009), precipitated as Sb_2S_3 (Zhang et al. 2016), or form mobile thioantimonate complexes (Ye et al. 2019). Direct transformations of Sb species by microorganisms include Sb(III) oxidation, Sb(V) reduction and methylation. More than 60 bacterial strains, belonging to 27 genera, presented the ability to enzymatically oxidise Sb(III) into Sb(V) (Deng et al. 2021). They may contribute to increasing the mobility of Sb from solid phases to water, in oxic and neutral pH conditions, as shown by Loni et al. (2020). Anaerobic bio-reduction of Sb(V) into Sb(III), involved in respiratory metabolism, has been evidenced with strains of *Sinorhizobium* (Nguyen and Lee 2014), *Desulfuribacillus* (Abin and Hollibaugh 2017), *Dechloromonas*, *Propionivibrio* (Yang et al. 2020) and *Geobacter* (Nguyen et al. 2018, Yamamura et al. 2021). Microbial methylation of Sb has also been shown to occur, particularly in reducing and organic matter-rich environments (Caplette et al. 2021). A few studies have reported microbiologically influenced Sb behaviour in environmental samples. Biotic versus abiotic incubations of sediments impacted by ancient mining activity indicated an effect of the microbial compartment on Sb release (Casiot et al. 2007) that increased in oxygenated conditions and decreased in anoxic conditions. This overview of the state of the art highlights the potential involvement of

a large range of microbial processes in either release of Sb from solid phases to water, or conversely, immobilisation of this toxic element in mineral sinks. However, considering the complexity of Sb geochemical behaviour, significant gaps still need to be addressed to evaluate the global resulting impact of biogeochemical processes, compared with non-biological mechanisms, in different environmental compartments of mining sites. The present study is aimed to: (1) evaluate the influence of microbial communities on Sb mobility from solid phases to water, in different surface compartments of a mining site, comparing oxidising versus reducing conditions; and (2) examine the composition and evolution of microbial communities in these different systems.

2. Material and Methods

2.1 Site description and sampling

Samples were taken from the abandoned Susana mine, located near La Puebla de Alcocer, Badajoz province, SW Spain (Fig. 1). Gumiel (1983) described this Sb mineralisation as a small vein-type deposit, exploited through two shallow shafts and galleries, with N130ºE direction, hosted by the Pre-Ordovician "*Complejo Esquisto Grauváquico*" (Lotze 1956), a monotonous succession of shales/schists and greywackes, where an important number of Sb mineralizations are present (Gumiel & Arribas 1987). The area lacks any remediation measures and presents abandoned mine waste dumps. These wastes are very heterogeneous in grain size, with frequent debris containing stibnite (Sb_2S_3), the only ore mineral recognised in mineralisation. There is no evidence of in situ ore processing actions, consequently the wastes correspond exclusively to non-processed materials.

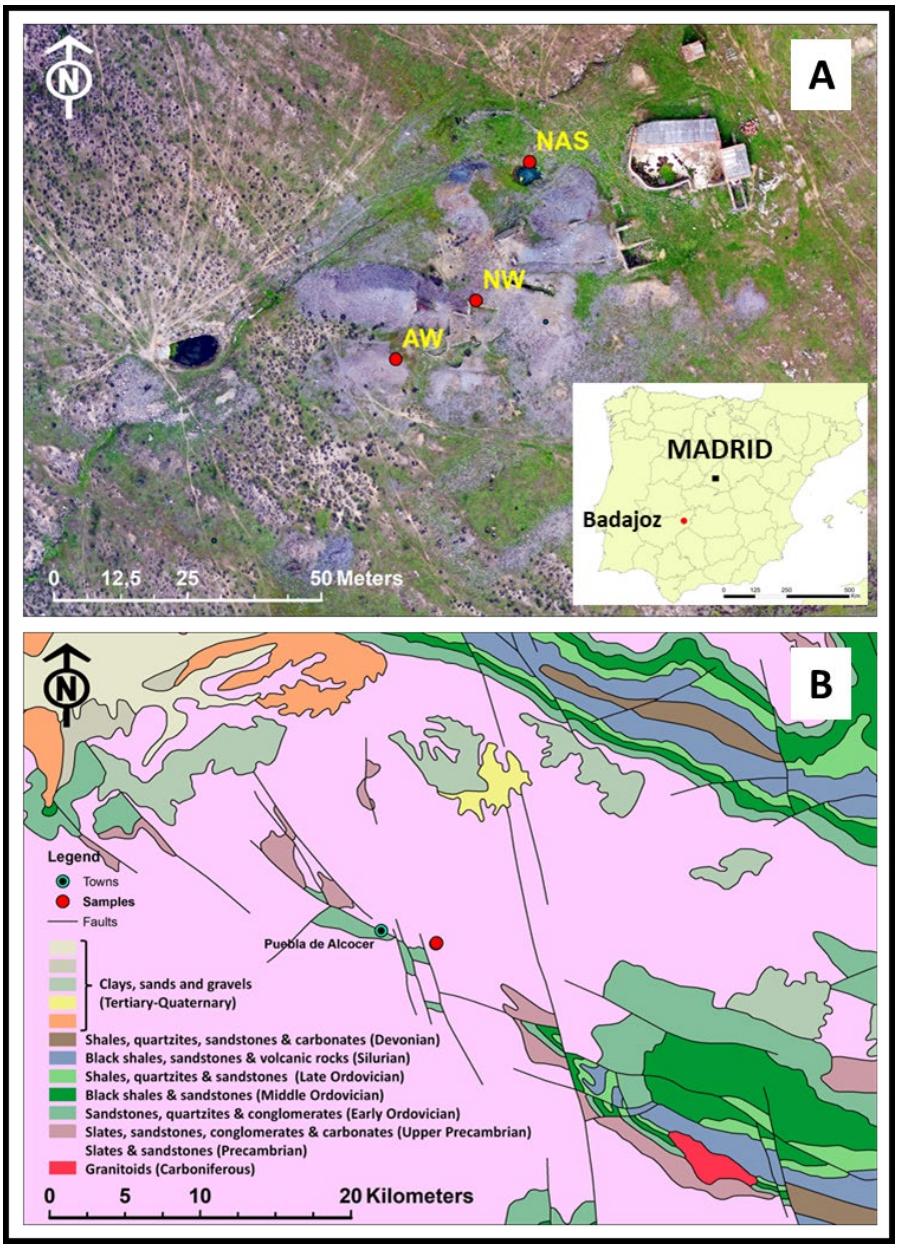

Figure 1. Presentation of the site, location (A); geological context (B)

From a climatic point of view, the area corresponds to the BSk Köppen climate (Cold semi-arid), which implies a dry area with low precipitation and extreme temperature conditions, particularly during winter. These conditions also imply a low degree of pedogenesis, and very poor vegetal cover, constituted by poor pastures and scattered presence of *Retama sphaerocarpa* bushes and the very occasional presence of acorn trees (*Quercus rotundifolia*).

Different constituents of the local landscape around the mine were sampled. Two samples were taken from a mine waste dump, including acidic pH waste (AW) and neutral pH waste (NW). The third sample corresponded to a sediment (NAS for neutral pH aquatic sediment) taken from a small, flooded area, some 1x1x1 meter in size, in which reducing conditions were suggested by a black substrate highly enriched in organic matter, and supporting an active population of tadpoles when the sampling was performed.

All samples were taken using plastic spoons, after homogenisation of the profile (0-15 cm deep) with a clean geologist's hammer and placed in plastic bags for transportation to the laboratory. Samples were air-dried at ambient temperature for 14 days, sieved to remove the <2 mm fraction, and split to obtain three subsamples: one to be stored, one for physicochemical determinations, and a last subsample to be milled for analyses. Non-dried samples were kept at 5°C in closed bags for incubation experiments.

2.2 Characterisation of solids

Preliminary analysis of the elemental composition of the samples was carried out by means of energy dispersive X-Ray fluorescence spectrometry (EDXRF), on milled samples, using an Epsilon 1 (from Malvern Panalytical). Mineralogical characterisation was performed using X-Ray diffractometry using a Bruker D8 Advance A25 in a 15-minute work program, on ground and pressed samples. Interpretation was carried out with Match! Software for phase analysis using powder diffraction data. Interpretation of diffractograms focused on the identification of the presence of quartz, Fe oxides and mineral phases containing Sb.

For incubation experiments, sub-samples of each material were subjected to autoclaving under N_2 atmosphere, three successive times at 120°C for 20 min, at 24 h intervals, in order to strongly attenuate microbial activity. This treatment did not kill 100% of the microorganisms; however, by convention the corresponding conditions are thereafter labelled as "Sterilised - St". In order to determine different mineral phases bearing Sb in soil samples

and to search for possible differences between autoclaved and non-autoclaved materials, 6 samples (3 autoclaved and 3 non-autoclaved) were analysed using SEM-EDS. The 6 soil samples were compressed using a hydraulic press (10 tons), each sample containing between 70 g and 110 g of material. The resulting samples were put into resin and thinly polished in order to be analysed using a ZEISS Merlin Compact Scanning Electron Microscope (SEM). The SEM was operated at 15KV, and it was provided with an EDXRF spectrum analyser (EDS, Bruker QUANTAX-XFlash6-30mm2-resolution 129eV), and a Bruker Micro XRF (XTRACE-Tube Rh-Filters Al, Ti, Ni). The results were analysed using ESPRIT Software.

Multielemental characterisation including total sulphur was carried out by EDXRF, using a Bruker S2 Ranger with a Pd detector with 10 g of ground and pressed samples.

Total organic carbon (TOC), humic and fulvic acids were analyzed according to the protocol described by Schnitzer (1983). For the determination of the TOC, 10 g of soil were added to 50 mL of extractant solution (44.6 g of 0.1 M pyrophosphate and 4 g of NaOH in a total volume of 1 L). Samples were shaken for 2 h and centrifuged for 15 min at 800 g. After that, 0.098 g of $K_2Cr_2O_7$ were added to 1 mL of the supernatant of the samples; then, 4 mL of concentrated H_2SO_4 were added and heated using a STUART SBH 200D/3 digester at 150ºC for 30 min. After 12 h, 5 mL of ultrapure H_2O were added, finally obtaining the result using a Spectronic UNICAM Helios Epsilon spectrophotometer at a wavelength of 590 nm. For the determination of humic and fulvic acids, 10 mL of the extract were taken and acidified with 0.2 mL of H_2SO_4. The samples were centrifuged for 15 min at 1,000 g. The resulting supernatant represents fulvic acids. Ten mL of NaOH 0.5 M were added to the resulting precipitate (humic acids). After stirring, 0.098 g of $K_2Cr_2O_7$ was added to 1 mL of the supernatant of the samples, and 4 mL of concentrated H_2SO_4 were added and heated using a STUART SBH 200D/3 digester at 150ºC for 30 min. After 12 h, 5 mL of ultrapure H_2O were added, and the solution was analysed at 590 nm using a Spectronic UNICAM Helios Epsilon spectrophotometer.

Evaluation of geochemical Sb mobility was performed through the following steps. The leachable fraction was evaluated using the Modified Geological Survey Field Leach Test

(Hageman 2007): 5 g of soil were mixed with 100 mL of deionised water shaken at 50 rpm for 2 h in a water bath. The supernatant was filtered through 0.45 µm PTFE filters. The available fraction was studied by means of $AcNH_4$ selective extraction: 5 g of soil were mixed with 100 mL of 1 M $AcNH_4$ solution at pH 7, shaken at 50 rpm for 2 h in a shaking water bath. The supernatant was filtered through a 0.45 µm PTFE filter. Modified BCR sequential extraction was carried out according to Quevauviller et al. (1997) in order to obtain data about fractionation of Sb and related elements. This sequential extraction procedure provides information about four fractions: fraction 1 (F1), extracted by a solution of 0.11 M acetic acid, releases the species that are soluble in water, easily leached by weak acids and associated with soluble carbonates; fraction 2 (F2), extracted by 0.5 M hydroxylamine hydrochloride, consists of easily reducible species associated with Fe and Mn oxy-hydroxides; fraction 3 (F3), extracted by 8.8 M hydrogen peroxide and 1.0 M ammonium acetate solutions, consist in easily oxidisable compounds, mainly associated with organic matter and sulphide minerals; and the residual fraction (RF) was determined by calculating the difference between pseudo-total and mobile fractions. A suitable certified reference material (BCR 701) was used to evaluate Pb recovery (between 95-98%). Extractions were filtered using Whatman filters (8 µm). The analysis of Sb, Pb, As, Fe, Mn and Cu in all solutions was performed by High-Resolution Atomic Absorption Spectrometry (HR-AAS), using an Analytik Jena ContrAA-800D.

2.3 Microcosms

Four types of microcosms were used: biotic and sterilised (St) in aerobic and anaerobic conditions. To establish the biotic microcosms, fresh samples (equivalent to 20 g dry weight) were mixed in sterile 500 mL glass bottles with 200 mL of sterilised Mont Roucous mineral water (composition close to rainwater, pH = 6.38, EC = 160 $\mu S.cm^{-1}$, Cl^- = 56 µM, NO_3^- = 24 µM, SO_4^{2-} = 16 µM, Na^+ = 109 µM, K^+ = 7.7 µM, Ca^{2+} = 25 µM, Mg^{2+} = 21 µM) and covered with cotton plugs (Ox: oxic conditions) or rubber stoppers (AOx: anoxic conditions). To create conditions with strongly attenuated microbial activities, bottles were prepared according to the

same protocol with St materials. At the beginning of the experiment and every week, 20 µl of formaldehyde was added to each St flask to prevent growth of the microorganisms that were not killed by autoclaving. All conditions were tested in triplicates, except the NAS St conditions, that were prepared in duplicates, due to the limitation of the quantity of material. In anoxic conditions, oxygen was purged from the microcosms with sterile N_2 for 20 minutes and pressurised with sterile H_2 (1 bar over atmospheric pressure). All microcosms were incubated for 41 days at 20ºC with rotational shaking (100 rpm) in the dark to prevent photo-induced oxidation of metals. Every week, samples were taken from the bottles and the water that evaporated in oxic conditions was compensated by adding sterile deionised water. For anoxic microcosms, sampling was conducted under strictly anaerobic conditions in an oxygen-free glove box and H_2 pressure was renewed after each sampling event.

2.4 Characterisation of water samples

At the beginning of the experiment and every week, one aliquot of the supernatant was sampled and pH, oxidation-reduction potential (ORP), electric conductivity (EC), Fe(II)/Fe(III) and Sb content were analysed. Additionally, Pb and As content were determined at the beginning, mid-time and end of the experiment. The pH, EC and ORP parameters were measured immediately in the suspensions using a Consort C3040 apparatus equipped with pH, ORP and EC electrodes. Supernatants were centrifuged at 10,000 g and filtered at 0.45 µm. For dissolved Fe speciation and quantification, a 1.5 mL aliquot was immediately acidified with concentrated HCl. Dissolved Fe(II) was measured using the ortho-phenantroline colorimetric method (Murti et al. 1966; Mamindy-Pajany et al. 2013). For this, 0.5 mL of acetate buffer pH 4.5, 0.1 mL of orthophenantroline 0.5 % and 0.9 mL of the filtered sample were added to a spectrophotometer cuvette. The mixture was left at room temperature for 15 min in the dark and the absorbance was recorded at 510 nm using a UV-Vis spectrophotometer. The total dissolved Fe concentration was determined using the same protocol but with the addition of 0.1 mL of hydroquinone 1 % prepared in acetate buffer pH 4.5. Samples for HR-AAS were

immediately acidified with 1 % of concentrated HNO_3. Concentrations of As, Sb and Pb were quantified by HR-AAS using a ContrAA-800 equipment (Analytik Jena, Germany) equipped with a xenon short-arc lamp and using the flame technique. All calibration standard solutions were prepared using 1 g L^{-1} primary certified standard solutions (Inorganic Ventures).

Speciation of Sb was determined at the end of incubation with the method described by Nguyen and Lee (2015) according to Yu et al. (2002). Samples were diluted in ultrapure water in order to reach a concentration lower than 250 µg L^{-1}. In glass tubes, 1 mL of sample was mixed with 3.5 mL of ultrapure water and 1 mL of 1 % pyrrolidine dithiocarbamate solution. After 10 min of reaction, the mixture was transferred to an Agilent SampliQ C18ODS (6 mL) solid-phase extraction cartridge, previously conditioned with 1 mL analytical grade methanol then 1 mL ultrapure water and placed above a collection tube. The cartridge was rapidly rinsed with 5 mL of ultrapure water, and Sb(III) was retained in the cartridge. Sb was quantified by oven Atomic absorption spectrometry (VARIAN) in the collection tube that received Sb(V) from the initial sample. The difference between total Sb and Sb(V) was considered to represent Sb(III).

2.5 Microbial growth and viability

The viability of microorganisms in each flask was determined at the beginning, mid-time and end of the incubation process, using a LIVE/DEAD® BacLight Bacterial Viability Kit (Molecular Probes 2004) to stain the bacteria fixed by filtration of 100 µL of incubated slurries diluted in 1 mL of sterile physiological water on GE Whatman™ Nuclepore polycarbonate membrane. Filters were observed under UV-light using a ZEISS Imager Z1 optical microscope (DSRED and FITC filters). Twelve images were taken in randomly chosen areas of each filter. Determination of live and dead cells was conducted by counting the number of green (live) and red (dead) points. Points were counted using a recorded macro in ImageJ (National Institute of Health, USA).

2.6 Characterisation of microbial communities

2.6.1 Extraction and quantification of soil DNA

DNA extractions were performed on initial soils and pellets obtained at the middle and end of the experiment after centrifuging the samples at 10,000 g. Pellets of triplicate microcosms were pooled before DNA extraction. Exclusively for the biotic AW in AOx conditions, DNA extraction and 16S fragment sequencing was also performed on individual replicates, because results in terms of Sb concentration strongly differed between these replicates. We used the FastPrep DNA Spin Kit for soil (MP Biomedicals) following the manufacturer's instructions. Total extracted DNA was quantified using a QUANTUS Fluorometer (Promega) and stored at –20 ºC until the next analysis.

2.6.2 16S rRNA amplification and next-generation sequencing

Bacterial and archaeal diversity was determined by 16S rRNA gene metabarcoding, generated by INRAE Transfert (Narbonne, France). The V4-V5 hypervariable region of the 16S rRNA gene was amplified using the barcoded, universal primer set 515WF/918WR (Wang et al. 2009). PCR reactions were performed using AccuStart II PCR ToughMix kit and cleaned (HighPrep PCR beads, Mokascience). Forward and reverse primers contained the adapter sequences (5'GTGYCAGCMGCCGCGGTA) and (3'ACTYAAAKGAATTGRCGGGG), respectively, used in Illumina sequencing technology. The amplicons were sequenced using an Illumina MiSeq at the GeT-PlaGe platform (Auzeville, France).

2.6.3 Processing of sequencing

The datasets from MiSeq sequencing were processing using the FROGS (Find, Rapidly, OTUs with Galaxy Solution) bioinformatics pipeline (Escudié et al. 2017). Fastq paired reads were merged with Vsearch software, and clustered into OTU (Operational Taxonomic

Units) with Swarm and an aggregation distance clustering of 1. Chimera and OTU with a proportion less than 0.0005% of all sequences were removed. Taxonomic affiliation was performed using BLAST and the Silva 138.1 database for 16S rRNA gene sequences. The raw datasets can be found on the European Nucleotide Archive system under project accession number **[in progress]**. InvSimpson diversity indexes were calculated based on the Illumina sequence data.

2.7 Statistics

Data about the evolution of soil microcosms were tested for homogeneity of variance and normal distribution. In this way, analysis of variance (ANOVA) was carried out using SPSS version 21.0 followed by a Tukey test between means of treatments to determine the significant difference ($p \leq 0.05$).

Redundancy analysis (RDA), using the vegan R package, was performed to identify the effects of environmental variables on bacterial phylum structure, based on the relative abundance of the detected OTU in pellets at t0, t21 and t41 days. This analysis was calculated based on a Hellinger-transformed phylum abundance basis of 16S rRNA data (Borcard et al. 2011). Environmental explanatory tested variables were standardised and the function ordistep in the vegan package was used to identify the significant explanatory environmental variables. The significance of the RDA model was tested by ANOVA based on the Monte Carlo test with 999 permutations. This analysis helps to determine the most influential factors and the extent to which different environmental parameters affected the bacterial phylum.

3. Results

3.1 Characterisation of solids

3.1.1. Mineralogy

The major Sb phases identified by XRD in rock samples from the site included stibnite (SbS_3) as the primary phase and stibiconite ($Sb^{3+}(Sb^{5+})_2O_6(OH)$ as the oxidised phase. However, in the soil and sediment samples used in this study, XRD analyses revealed only an oxidised phase of Sb and As, stenhuggarite $CaFeSb(AsO_3)_2O$ (5.3% in NAS sample), in addition to quartz as the majority phase (95-99%) and Fe and Mn oxides (5.6% in AW sample).

According to the SEM-EDS observations (Supplementary Table 1 and Supplementary Fig. 1), the most frequently observed Sb-bearing mineral phases are stibnite (in all samples), and Sb-oxides, including cervantite ($Sb^{3+}Sb^{5+}O_4$), bindheimite ($Pb_2Sb_2O_6(O,OH)$, and other Sb-oxides that would need further studies to be more precisely determined. Jamesonite (Pb_4FeSb_6S) is also present in lesser quantities. Besides these Sb-containing minerals, other important minerals present in both St and non-St samples–include quartz, rutile, Fe oxides (hematite), arsenopyrite, and monazite. Regarding Sb-bearing minerals, no significant difference was found between St and non-St samples through these qualitative analyses. Nevertheless, a detailed quantitative study of the Sb-oxides might lead to some important differentiation.

3.1.2 Chemical composition

All samples are siliceous, with variable contents of Fe (4.6-16.5 %), Sb (1.02-4.41 %) and As (878-9,800 mg kg^{-1}), as shown in Table 1. The NAS sample clearly differs from the other samples, especially in terms of higher concentrations of Fe, As, TOC (Table 1), P, Mn, Cr and Ca (Supplementary Table 2).

318 **Table 1.** Characteristics of initial materials. All data are expressed in %. (*) % of TOC

	AW	NW	NAS
Fe	4.61	4.67	16.49
Sb	4.41	1.02	1.08
S	0.53	0.13	1.11
As	0.22	0.09	0.98
TOC	2.35	2.43	9.59
Humic Acid	0.89 (37.8%)*	1.29 (53.1%)*	2.65 (27.6%)*
Fulvic Acid	1.46 (62.1%)*	1.14 (46.9%)*	6.94 (72.3%)*

319

320 **3.1.3 Geochemical mobility of Sb**

321 A clear differentiation was found in the fractionation between different samples and
322 different considered elements. The first noteworthy finding is the overwhelming proportion of
323 Sb in the residual phase in all samples, although the proportion of Sb in more available phases
324 is very slightly higher in the NAS sample (Supplementary Figure 2). This is confirmed by the
325 negligible proportion of Sb extracted in a leaching test, or even extracted with $AcNH_4$
326 (Supplementary Figure 2A). The fraction extracted with $AcNH_4$ tends to be higher in the AW
327 sample than in the NAS sample. With the BCR protocol, Fe is extracted in higher proportions
328 (more than 40%) in the soluble/available fractions (Supplementary Figure 2B) only in the NAS
329 sample, with the highest values corresponding to the F2 fraction linked to Fe and Mn oxides.
330 However, the low proportion of extracted Sb in F2 suggests that most of the Sb is not
331 associated with oxides in the NAS sample. Iron is only present in very small proportions as
332 oxides in the NW and AW samples.

333

334 **3.2 Microcosms**

335 **3.2.1 Evolution of physico-chemical parameters**

336 In the AW microcosms, oxidising conditions with microbial growth produced a strong
337 release of Sb (≈ 495 % of the initial concentration, Fig. 2A). However, under anoxic conditions,

the three replicates in biotic conditions behaved differently (Fig. 2B): Sb was released more in solution than in the St condition for replicate A, but immobilised between days 6 and 15 in replicate B and immobilised from the beginning of incubation in replicate C. In all replicates, a late release of Sb into water was observed during the last week of incubation. Few changes were observed in the St microcosms. On the other hand, in NW microcosms (Fig. 2C), a release of Sb was observed in all cases (452 % Ox, 283 % Ox St, 353 % AOx St), although it was much less pronounced in the AOx microcosm (92 %). Regarding NAS microcosms (Fig. 2D), a release was observed in all cases; however, it was much stronger in the St microcosms than in the biotic microcosms for both Ox and AOx conditions (58 % Ox, 122 % Ox St, 131 % AOx, 152 % AOx St). More precisely, in oxic conditions Sb was released more in biotic than in St conditions during the first week, then the Sb concentration decreased sharply between day 6 and day 13. Arsenic had a more homogeneous behaviour within the three studied materials (AW, NW and NAS, Table 1 and Supplementary Fig. 3). In all cases, the microcosm under anoxic conditions and with microorganisms produced a release of the metalloid, while in the rest of the microcosms the release was lower. No release of Fe(III) was observed in any of the microcosms (data not shown). However, under anoxic and biotic conditions, an increase in the content of soluble Fe(II) could be observed mainly with AW and a few with NW, while in the rest of the microcosms it remained almost unchanged (Fig. 3).

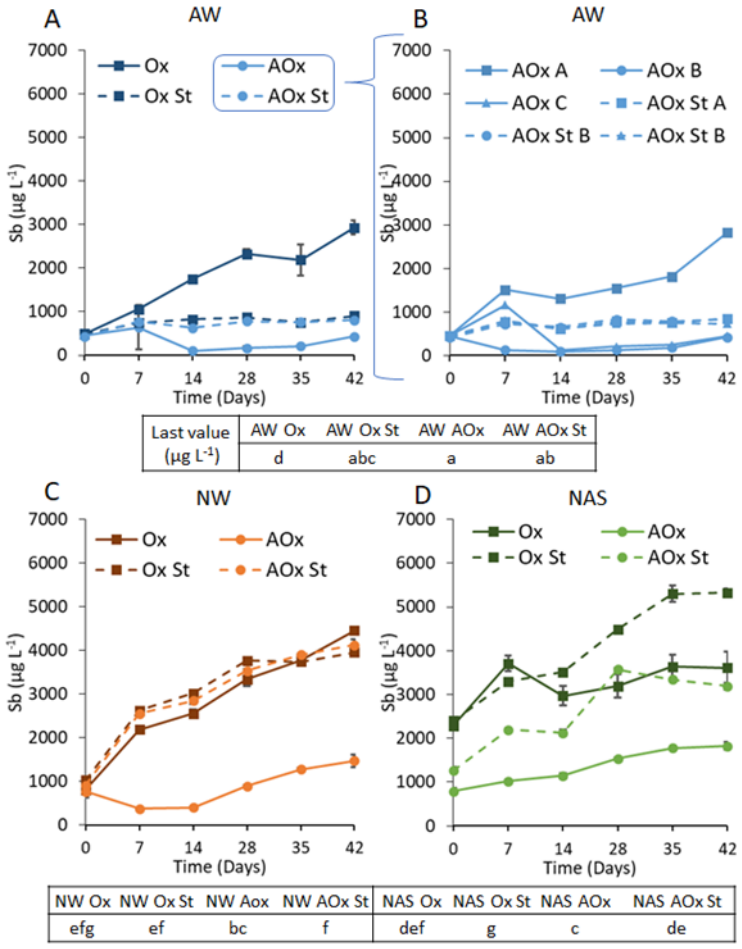

356

357 **Figure 2.** Evolution of Sb concentration in the liquid phase of acidic pH waste (AW, A & B),
358 neutral pH waste (NW, C) and neutral pH aquatic sediment (NAS, D) microcosms. Ox (oxic-
359 biotic conditions), Ox St (oxic-abiotic conditions), AOx (anoxic-biotic conditions) and AOx St
360 (anoxic-abiotic conditions). Values show the mean of three replicates ± SE. Values with the
361 same small letters are not significantly different at $P \leq 0.05$ (ANOVA, Tukey test).

362

363 AW microcosms showed lower pH as compared to the other two soil types (NW and
364 NAS, Supplementary Fig. 4). In the AW microcosm with microorganisms, the pH decreased in
365 Ox conditions and increased in AOx conditions, whereas no change of pH was observed in
366 abiotic conditions. With NW, pH increased in AOx conditions while no major pH change was
367 observed in the other conditions. Similar behaviour was observed in NAS, where an increase
368 in pH was observed only under AOx conditions with microorganisms. The ORP evolved

similarly for all materials (AW, NW and NAS, Supplementary Fig. 5): it reached values of around 200-300 mV (Ref. Ag/AgCl) in microcosms under Ox conditions, while in AOx conditions it decreased down to -300 mV, with no clear influence of living microbes in any condition.

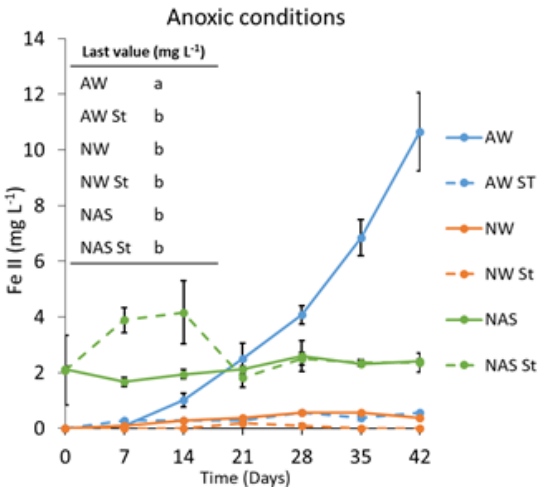

Figure 3. Evolution of Fe(II) concentration in reducing conditions of acidic pH waste (AW, A), neutral pH waste (NW, B) and neutral pH aquatic sediment (NAS, C) microcosms. St indicates abiotic conditions. The Fe(II) concentration did not vary under oxidising conditions. Values show the mean of three replicates ± SE. Values with the same small letters are not significantly different at $P \leq 0.05$ (ANOVA, Tukey test).

The monitoring of EC showed differences between the studied microcosms (Supplementary Fig. 6). A very strong increase of EC was observed in AW and NAS incubated in Ox conditions with microorganisms (400% and 162%, AW and NAS, respectively), whereas with NAS, EC tended to decrease in biotic AOx microcosms. In the NW microcosm, there was only a slight increase over the weeks in all conditions.

The final speciation of Sb in the water phase (Table 2) showed the dominance of Sb(V) in all conditions, except in the biotic AOx incubations of NW, in which Sb(V) represented only 20 to 30% of total Sb.

388

389 **Table 2.** Speciation of Sb, total Sb and total As in the water phase at the end of the incubation
390 experiment (day 42).

Condition	Replicates	Total Sb (µg L^{-1})	Sb(V) (µg L^{-1})	Sb(V) (%)	Total As (µg L^{-1})
AW Ox	A	2231	2030	91	208
	B	2657	2475	93	217
	C	2693	2253	84	240
AW Ox St	A	1316	1205	92	256
	B	887	768	87	265
	C	1507	1368	91	304
AW AOx	A	3516	3318	94	1337
	B	664	559	84	2955
	C	576	353	61	2963
AW AOx St	A	1049	819	78	360
	B	992	816	82	322
	C	943	752	80	249
NW Ox	A	4596	3981	87	908
	B	4898	4175	85	850
	C	5320	4847	91	892
NW Ox St	A	4030	3691	92	650
	B	3950	3547	90	839
	C	3534	3216	91	854
NW AOx	A	2039	629	31	9764
	B	2199	649	30	10540
	C	2184	440	20	10676
NW AOx St	A	4250	3696	87	1146
	B	4552	3960	87	1109
	C	4370	3985	91	1069
NAS Ox	A	3200	3059	96	118
	B	3758	3564	95	116
	C	2652	2424	91	95
NAS Ox St	A	5516	5108	93	1250
	B	4474	4083	91	1764
NAS AOx	A	2021	1453	72	15045
	B	1808	1539	85	14986
	C	2155	1482	69	15515
NAS AOx St	A	3756	3356	89	2285
	B	2816	2561	91	2216

391

392 **3.2.2 Evolution of the microbial compartment**

393 The cell density increased in all incubation conditions (Fig. 4), the highest cell
394 concentrations being found in the NAS. This result was in accordance with the DNA
395 quantification data (Supplementary Table 3). For AW microcosms, the AOx conditions gave
396 the highest abundance of live cells: however, in NW there was a similar abundance of living
397 cells in Ox and AOx, and in NAS more living cells were found in Ox at the end of incubation

(Fig. 4 A, B and C). Considering dead cells, their abundance in AW was similar between Ox and AOx conditions; however, in NW and NAS materials, dead cells were more abundant under AOx conditions (Fig. 4 D, E and F). Cells (live and dead) were observed in St conditions, however, low DNA concentrations confirmed that growth in the presence of St materials was limited.

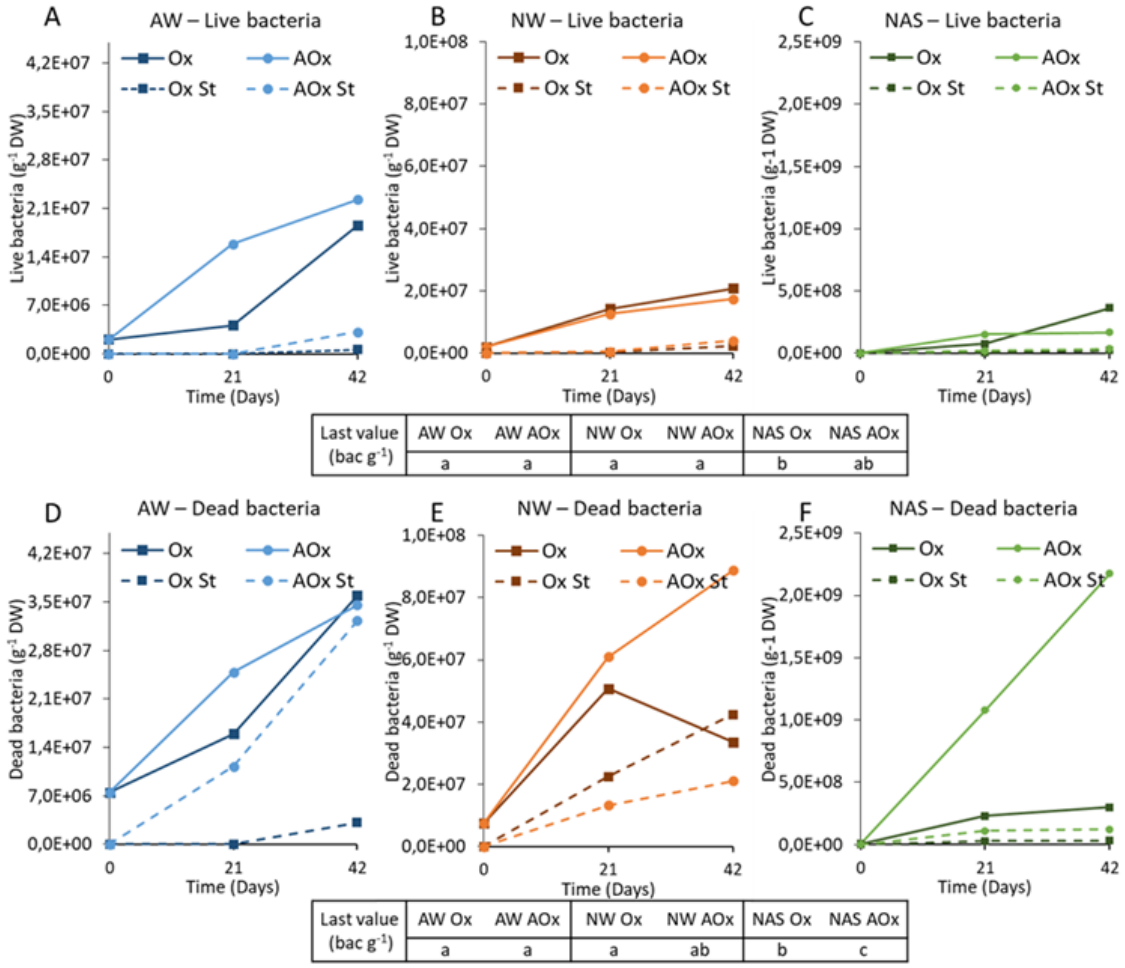

Figure 4. Evolution of live and dead cells abundance (cells g^{-1} of solid dry weight) in acidic waste (AW, A & D), neutral waste (NW, B & E) and neutral aquatic sediment (NAS, C & F) microcosms. Ox (oxic-biotic conditions), Ox St (oxic-abiotic conditions), AOx (anoxic-biotic conditions) and AOx St (anoxic-abiotic conditions). Values show the mean of three replicates ± SE. Values with the same small letters are not significantly different at $P \leq 0.05$ (ANOVA, Tukey test).

A total of 382,567 sequences of 16S rRNA gene were obtained from the 21 samples. The highest richness was observed in the NAS (Supplementary Figure 7). It ranged from 657 OTUs in the soil at the beginning of experiment (t0) to 570 in the Ox condition after 42 days. In NW, 514 OTUs were observed at t0. This sample shows the greatest difference between the Ox and AOx conditions: after 21 days, in AOx conditions, the richness decreased to 321 before increasing to 508 at the end. The lowest richness was observed in AW with a number of OTUs between 300 and 400. OTUs were observed in St conditions: with AW and NAS, few OTUs were present at the end of the St experiment however in NW about 400 OTUs were observed in both St conditions. The diversity based on the InvSimpson index decreased in all conditions between 0 and 21 days, except for NW Ox and AW Ox conditions (Supplementary Figure 7). Between 21 and 42 days, the diversity increased in NW Ox and NAS AOx, and decreased in AW Ox. At the end of the experiment, diversity was higher in the Ox condition than in the AOx condition for AW and NAS, but higher in the AOx than in the Ox condition for NAS. Diversity in the St conditions was very low, except for the NAS condition, where it was close to the biotic condition.

The relative abundance of the major bacterial and archaeal phyla is shown in Fig. 5. AW was characterised by a predominance of Chloroflexi. Ox conditions favoured the development of Proteobacteria, Bacteroidota, Planctomycetota, Cyanobacteria, and WPS-2, while AOx conditions promoted the development of Firmicutes (which became the main phylum) and Acidobacteria. NW was dominated by five phyla: Proteobacteria, Actinobacteriota, Acidobacteriota, Bacteroidota, and Crenarchaeota. Ox conditions enhanced the development of Proteobacteriota and Bacteroidota, whereas Firmicutes, Desulfobacterota and Myxococcota emerged in AOx conditions. Quite similar compositions at the phylum level were observed in NW and NAS; however, three phyla were important in this sediment: Desulfobacterota, Myxococcota, and Halobacterota. As observed in NW, Proteobacteria and Bacteroidota abundance increased in NAS microcosms with Ox conditions, but a decrease in abundance of Firmicutes, Desulfobacterota, and Halobacterota was also observed. In AOx

conditions, the NAS phylum composition was very similar during the experiment with no major variations. The main phyla observed in AW and NAS St conditions were Proteobacteria and Actinobacteria, meanwhile Firmicutes, Acidobacteriota, and Bacteroidota were also observed in proportions greater than 5% in NW.

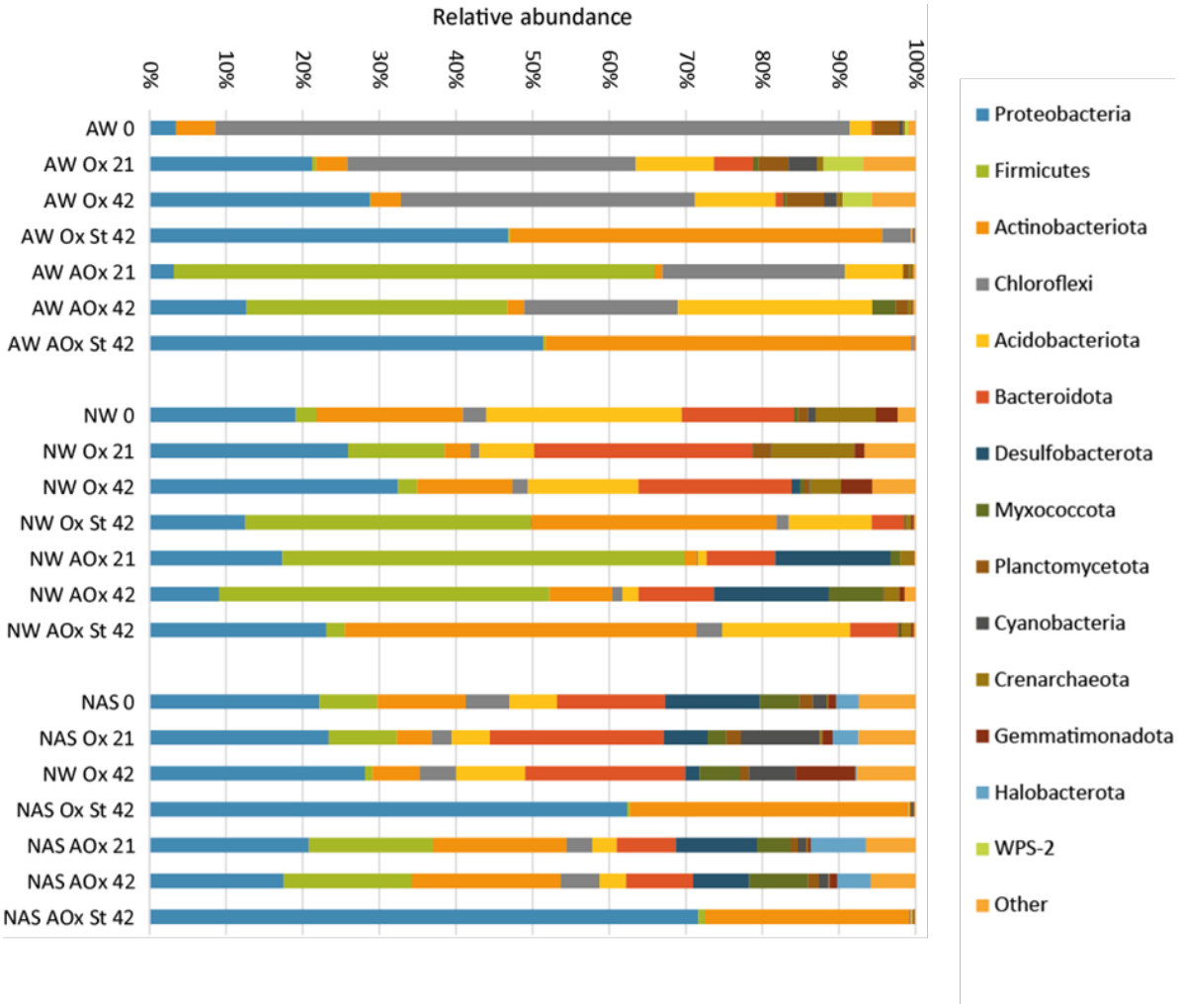

Figure 5. Relative abundance of the major bacterial and archaeal phyla in soils and samples from acidic pH waste (AW), neutral pH waste (NW) and neutral pH aquatic sediment (NAS) microcosms. Ox (oxic-biotic conditions), Ox St (autoclaved oxic-abiotic conditions), AOx (anoxic-biotic conditions) and AOx St (autoclaved anoxic-abiotic conditions).

With the aim of identifying the influence on the microbial community structure of the physico-chemical characteristics of the sampled water, an RDA was built (Fig. 6). The results indicate that pH and ORP were explanatory variables that significantly influenced the

community structure at the phylum level, explaining 24 % (p = 0.009) of the total variance. The lowest pH favoured the presence of Chloroflexi, whereas high pH seemed to induce higher proportions of Desulfobacterota and Bacteroidota. Low ORP, in AOx conditions, favoured the development of Firmicutes. The St conditions had the same community structure, regardless of their conditions, except for the NW Ox condition.

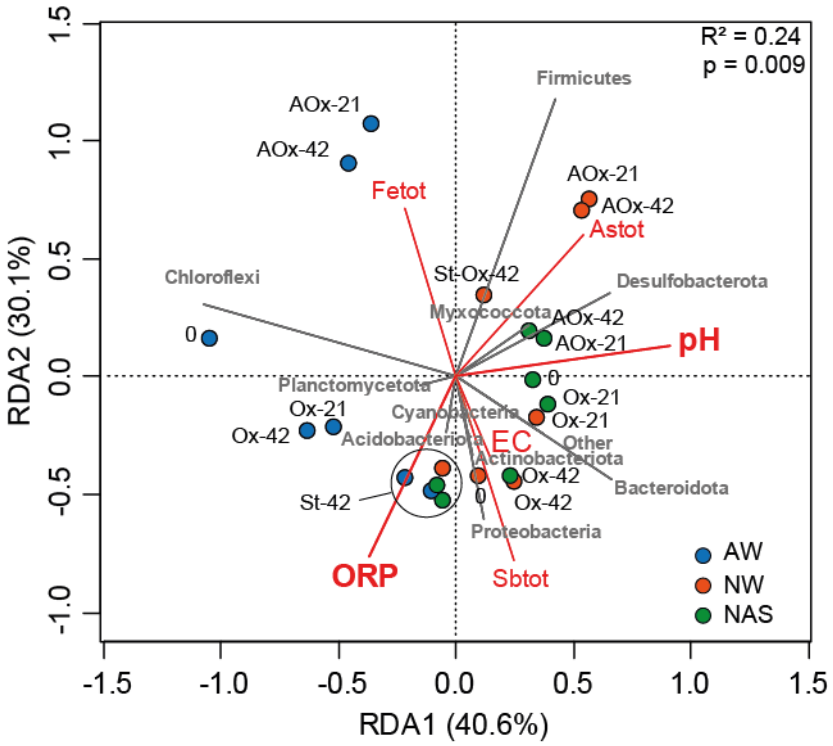

Figure 6. RDA of sequence abundances assigned at phylum level of bacterial and archaeal communities in soils and microcosm samples in relation to environmental variables. Red lines represent the environmental variables (significant variables in bold), grey lines represent the Phyla, and circles represent the samples (AW in blue, NW in red and NAS in green). Ox (oxic-biotic conditions), Ox St (autoclaved oxic-abiotic conditions), AOx (anoxic-biotic conditions) and AOx St (autoclaved anoxic-abiotic conditions).

Some of the OTUs identified at the genus level correspond to genera that were shown to be involved in the metabolisms of Sb, S or Fe (Table 3). Their proportion in the total number of sequences for each sample, grouped by common metabolism, strongly varied between

conditions (Fig. 7). With the AW, these metabolic groups represented a very low proportion of the sequences in oxic conditions, whereas in anoxic conditions, Sb(III)-oxidising, sulphate-reducing bacteria (SRB) and Fe(III)-reducing groups emerged during incubation. At the end of the experiment (day 41), the two replicates AOx B and AOx C, in which Sb was immobilised, counted more Fe(III)-reducing bacteria and SRB, and fewer genera including Sb(III)-oxidising strains than the replicate AOx A, in which Sb mobility was higher. This result could be linked to the higher proportion of Sb(V) in AOx A than in AOx B and C (Table 2). With the NW, a high proportion of the Sb(III)-oxidising group was observed in oxic conditions, particularly in the St conditions, linked to the high proportion of sequences affiliated to the genera *Bacillus* and *Novosphingobium* in these samples (Supplementary Table 4). However, this might not lead to any biogeochemical interpretation, as biomass was very low in the St conditions (Supplementary Table 3). In anoxic conditions, NW was enriched in Sb(V)-reducing and Fe(III)-reducing metabolic groups, with a major contribution of *Geobacter* in these two groups (Supplementary Table 4). Sulphate-reducers also emerged in the NW biotic AOx incubation, to a lesser extent. With the NAS, the targeted metabolic groups did not appear in the St conditions, whereas, with the exception of the Sb(V)-red group, they were well represented in all the biotic conditions, even at t0. Incubation conditions seemed to favour the development of Sb(III)-oxidising and SOX groups in oxic conditions, and of Sb(III)-oxidising and more clearly Fe(III)-reducing groups in anoxic conditions, with *Anaeromyxobacter* and *Geothermobacter* as the main corresponding putative Fe(III)-reducers (Supplementary Table 4).

492 **Table 3.** List of genera including strains with known metabolisms related to the biogeocycles
493 of Sb, S or Fe and detected in Susana sample incubations. Acidic pH waste (AW), neutral pH
494 waste (NW) and neutral pH aquatic sediment (NAS). Ox: oxic; AOx: anoxic; St: sterilised
495 conditions.

Genus	Metabolisms	Detected in	Reference
Cupriavidus	Sb(III)-oxidising	NW: AOx, AOx St	Nguyen and Lee 2015
Pseudomonas	Sb(III)-oxidising	AW: OxSt NW: Ox, OxSt, AOx, AOx St	Nguyen and Lee 2015
Bacillus	Sb(III)-oxidising	AW: Ox, OxSt, AOx, AOx St NW: Ox, OxSt, AOx, AOx St, NAS: Ox, AOx	Li et al. 2018
Bosea	Sb(III)-oxidising	NW: Ox, OxSt, AOx, AOx St	Xiang et al. 2022
Acidithiobacillus	Sb(III)-oxidising	AW: OxSt, AOx, AOx St	Nguyen and Lee 2015
Flavihumibacter	Sb(III)-oxidising	NAS: Ox, AOx	Han et al. 2016
Hydrogenophaga	Sb(III)-oxidising	NAS: Ox, AOx	Terry et al. 2015
Novoshingobium	Sb(III)-oxidising	NW: Ox, OxSt, AOx, AOx St NAS: Ox, AOx, AOx St	Deng et al. 2021
Thiobacillus	Sb(III)-oxidising S-oxidising	AW: OxSt, NW: Ox, NAS: Ox, AOx	Deng et al. 2021
Roseomonas	Sb(III)-oxidising	AW: OxSt NAS: Ox, AOx	Sun et al. 2020
Geobacter	Sb(V)-reducing Fe(III)-reducing	AW: OxSt NW: Ox, AOx NAS: Ox, AOx	Nguyen et al. 2018
Thermithiobacillus	S-oxidising	AW: Ox	Yang et al. 2015
Acidithiobacillus	S-oxidising Fe(II)-oxidising	AW: Ox St, AOx, AOx St NW: AOx St NAS: AOxSt	Quatrini and Johnson 2019
Sideroxydans	Fe(II)-oxidising	AW: Ox St NAS: Ox, Ox St, AOx	Weiss et al. 2007
Gallionella	Fe(II)-oxidising	NAS: Ox, AOx	De Vet et al. 2011
Anaeromyxobacter	Fe(III)-reducing	AW: AOx, Ox St NW: AOx NAS: Ox, AOx	Treude et al. 2003
Geothermobacter	Fe(III)-reducing	NAS: Ox, AOx, AOx St	Kashefi et al. 2003
Desulfitobacterium	Fe(III)-reducing, S-reducing	AW: AOx, ZOx St NW: Ox, AOx NAS: Ox, Ox St AOx	Finneran et al. 2002
Desulfosporosinus	S-reducing	AW: Ox, AOx NW: Ox, AOx NAS: Ox, AOx, Ox St	Alazard et al. 2010
Desulfatirhabdium	S-reducing	NAS: Ox, AOx	Balk et al. 2008
Desulfotomaculum	S-reducing	NW: AOx NAS: Ox	Kaksonen et al. 2004
Desulfurivibrio	S-reducing	NAS: AOx	Kaksonen et al. 2004
Desulfobulbus	S-reducing	NAS: Ox, AOx	Kaksonen et al. 2004
Desulfovirga	S-reducing	NAS: Ox, AOx	Deng et al. 2016
Syntrophobacter	S-reducing	NAS: Ox, AOx	Sánchez-Andrea et al. 2012

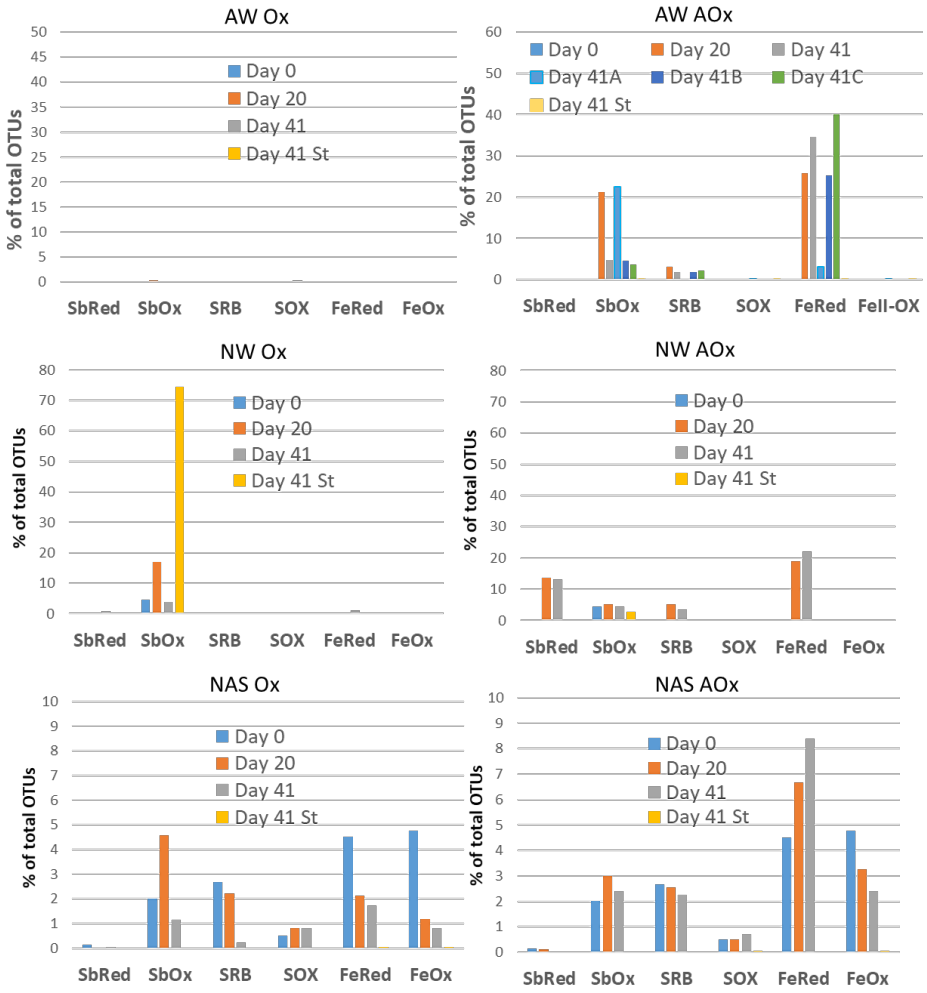

Figure 7. Proportion in each sample, according to the obtained 16S sequences, of the sum of identified genera including Sb, S or Fe-transforming bacterial strains, grouped according to metabolic processes. Incubations of acidic pH waste (AW), neutral pH waste (NW) and neutral pH aquatic sediment (NAS). Ox: oxic; AOx: anoxic; St: sterilised conditions. SbRed: Sb(V)-reducing; SbOx: Sb(III)-oxidising, SRB: sulphate-reducing bacteria; SOX: Sulphur-oxidising; FeRed: Fe(III)-reducing; FeOx: Fe(II)-oxidising. Genera included in each group are detailed in Table 2.

4. Discussion

4.1. Evolution of Sb concentrations

Dissolved Sb concentrations in the present experiments varied from 90 µg L^{-1} (in the AW biotic anoxic conditions) to 5,400 µg L^{-1} (in the NAS St oxic condition). These values are in the range previously found in mining environments, i.e. 2,200 µg L^{-1} in the adit of Goesdorf mine, Luxembourg (Filella et al. 2009); 1,600 µg L^{-1} in a pond receiving water from tailings of the Giant gold Mine in Yellowknife, Canada (Fawcett et al. 2015); from 2,900 µg L^{-1} in surface water to 23,000 µg L^{-1} in groundwater from Xikuangshan mine, China (Wen et al. 2016).

The mobility, bioavailability, and transport of Sb in soils are directly linked to its speciation as well as to the pH, redox conditions, type of minerals and microbial processes (Pitman et al. 1957; Fillela et al. 2002; Wilson et al. 2010; Herath et al. 2017). Different behaviours of Sb were observed with our three studied materials presenting different pH values. Considering the results of the St microcosms, while in the AW (pH $\simeq$ 4) the dissolved Sb concentration remained unchanged, in NW and NAS (pH $\simeq$ 6.5) there was an increase in soluble Sb concentration. Whereas sequential extractions showed that most Sb is present in forms that are resistant to dissolution, the high total Sb concentration in all materials explains the dissolved Sb concentrations observed in the microcosms. Experiments carried out by Hu et al. (2016) showed different effects of pH on Sb release from mining soils, depending on mineralogy. Here, the three analysed materials contained stibnite and Sb oxides (Supplementary Table 1). Stibnite dissolves in oxygenated water to form the hydroxide $Sb(OH)_3$ (Biver and Shotyk 2012). The corresponding dissolution rate is lower at near neutral pH than in acidic or alkaline conditions, thus this reaction could hardly explain our results in St condition. The resulting hydroxide $Sb(OH)_3$ presents a low solubility, as it can form a solid species $Sb(OH)_3(s)$ (Brookins 1986; Shkol'nikov 2010). Our materials also contained Sb oxides, that might dissolve in aqueous solutions producing the Sb(V) species $Sb(OH)_6^-$, which can exist over a wide range of pH (Pitman et al. 1957; Brookins 1986) including our experimental conditions, and the poorly soluble $Sb(OH)_3$. As a matter of fact, in St conditions,

Sb was mainly present as Sb(V) at the end of incubation (Table 2), even in anaerobic conditions, suggesting a phenomenon linked to the abiotic dissolution of Sb(V)-containing minerals. Thermodynamic equilibrium data indicate that Sb(V) species should exist in aerobic conditions and Sb(III) species in anoxic and low-redox environments (Pitman et al. 1957; Filella et al. 2002), however the presence of oxidised Sb species in anaerobic systems has already been observed (Fillela et al. 2002; Mitsunobu et al. 2006; Fawcett et al. 2015), suggesting the major role of kinetics in Sb speciation, that could be influenced by microbial catalysis phenomena. As a fact, we observed important differences in ORP (Supplementary Fig. 5) that did not induce differences in Sb concentrations (Fig. 2) in St conditions, whereas the redox conditions significantly influenced Sb behaviour in presence of microbes and the microbial communities (Fig. 6). Also, the adsorption and desorption of Sb by oxyhydroxides control its concentration in solution. Oxyhydroxides have strong affinity for Sb; however, adsorption efficiency depends on their type, pH and Sb species (Kong et al. 2016; Wang et al. 2021). The presence of Mn-, Fe- and Al oxyhydroxides affects the fate of Sb through sorption and oxidation and its affinity for Sb is affected by pH (He et al. 2019). Acidic pH conditions favour the sorption of both Sb(III) and Sb(V) onto Mn- (Wang et al. 2021), and Fe- (Leuz et al. 2006) oxides, with the rate of sorption decreasing subsequently with the increase in pH. These results appear consistent with those obtained in our study, where the most acidic material (AW St) released less Sb in solution than the other two studied materials (NW St and NAS St). Iron oxides were detected in most materials through mineralogical analysis (supplementary Table 1) and chemical extractions (Supplementary Fig. 2). The biogeochemical behaviour of Fe is strongly influenced by pH (Emerson and Weiss 2004), Fe(II) solubility being increased in low pH conditions (Frohne et al. 2011). This fact could explain the increase in soluble Fe concentration under reducing conditions in AW (Fig. 3), since it could be attributed to the bio-reduction of Fe hydroxides. However, Sb was rather immobilised than solubilised in the corresponding microcosm. These results suggest that adsorption/desorption mechanisms linked to Fe oxides were not the only processes controlling the fate of Sb in our microcosms.

4.2. Significance of the comparison biotic *vs.* St conditions

Through the present experiments, it was possible to evaluate the influence of microbial activities on the mobility of Sb in diverse surface compartments of a mining site, through comparison of complete microbial communities with systems in which microbial activities were greatly weakened. There is no efficient way to completely sterilise environmental samples (Otte et al. 2018). Here, the autoclaving of materials in anoxic conditions did not seem to strongly alter minerals, whereas it could have impacted the organic compartment, in particular in the NAS. Monitoring of cell densities by the LIVE/DEAD® BacLight Bacterial Viability Kit showed higher cell concentrations in anoxic conditions than in oxic conditions. Abundant growth in anoxic conditions could be linked to the availability of H_2 that could be used as an energy source. Dominance of “dead” cells in these samples might simply result from the experimental procedure as filtration and staining were performed in an oxygenated atmosphere. However, “live” cells were also observed in all incubations and their concentration increased, indicating active microbial metabolisms. Conversely, low cell counts, and low final DNA concentrations, indicated that autoclaving and formaldehyde injections greatly weakened microbial metabolism in the St conditions.

4.3. Role of microbial communities

4.3.1. Comparison of environmental compartments

Microbial communities presented very different compositions depending on the type of material, AW, NW or NAS, suggesting a diversity of biological processes depending on environmental compartments at the site. Interestingly, a few OTUs identified at the genus level that were retrieved in most of the samples, such as *Bacillus*, *Desulfosporosinus* and *Desulfitobacterium*, correspond to spore-forming microorganisms, able to resist adverse conditions. Not surprisingly, the most acidic environment presented the lowest diversity, and pH was one of the parameters influencing microbial communities’ structure. Previous studies showed that Sb contamination could influence the composition of microbial communities on

588 mining sites (Deng et al. 2020; Duan et al. 2022). In sediments of a watershed contaminated
589 by Sb mining, pH, temperature, ORP and dissolved Sb significantly structured the microbial
590 communities (Sun et al. 2016). Here, we observed strong divergences between communities
591 of surface environments at a small site scale that seemed to be more influenced by pH and
592 redox conditions than by soluble Sb.
593
594 **4.3.2. Bio-processes in oxic conditions**

595 Previous studies have already shown that microbial activities could influence the
596 mobility of Sb. Casiot et al. (2007) observed that Sb release from a sediment polluted by mining
597 activities was enhanced by aerobic microbial activity and attenuated in anoxic biotic conditions.
598 Loni et al. (2020) observed higher Sb solubilisation from mining rock samples, in oxic
599 conditions, by an Sb(III)-oxidising micro-organism affiliated to the *Paracoccus* genus. Here, in
600 the presence of oxygen, the overall effect of microbial processes differed between the types
601 of materials: Sb release was enhanced by biological processes in the AW, not influenced in
602 the NW, and attenuated in the NAS.

603 In AW, microbial activities in oxic conditions promoted Sb release and acidification;
604 however these processes could not be clearly related to the analysis and evolution of the
605 microbial community, that was largely dominated by OTUs belonging to Chloroflexi of the
606 family of Ktedonobacteraceae, none identified at the genus level. This family includes
607 filamentous, spore-forming, gram-positive heterotrophic bacteria from soil (Cavaletti et al.
608 2006). However, although limited (0.6% of total OTUs on day 41), emergence of the known S-
609 oxidising genus *Thermithiobacillus* was observed in these microcosms. The observed
610 biologically-related release of Sb from AW might be related to the direct or indirect alteration
611 of Sb-bearing phases, such as sulphides or organic matter. In NW, biological activities did not
612 significantly influence Sb mobility in oxic conditions, and no known genus with metabolisms
613 based on Sb, S or Fe transformations was identified in the microbial communities that seemed
614 dominated by heterotrophic phyla. Conversely, the NAS incubated in oxic conditions showed

615 an overall immobilisation of Sb in biotic compared with St conditions, but only after a strong
616 release of Sb that was observed in both conditions during the first week of incubation. These
617 results could be explained by the early oxidation of amorphous Fe sulphide, often present in
618 aquatic sediments (Andrade et al. 2010), that would release Fe(II), (bio)-oxidised into Fe(III),
619 that would rapidly precipitate as fresh Fe oxides known to adsorb Sb (Ashley et al. 2003). The
620 increase in the proportion in S-oxidising genus *Thiobacillus* between T0 and T20 days, and the
621 presence of the Fe(II)-oxidising genera *Sideroxydans* and *Gallionella* in the sediment appear
622 to be in agreement with this hypothesis. The observation of a colour change, from dark brown
623 (St condition) to ochre-brown (biotic condition) also supported this scenario (Supplementary
624 figure 8A). Moreover, the pH values that were lower in NAS than in NAS St, possibly linked to
625 biologically-induced reactions (Fe hydroxydes precipitation, oxidation of sulphur compounds,
626 oxidation of organic matter producing CO_2), could favour Sb adsorption onto oxides (Leuz et
627 al. 2006).

628

629 **4.3.2 Bio-processes in anoxic conditions**

630 In the microcosms, Sb release was nearly always attenuated by living micro-organisms
631 in anaerobic conditions. However, with the AW incubated in AOx conditions, the three
632 replicates behaved differently in terms of Sb mobility and microbial communities. In two
633 replicates, Sb was immobilised compared with the St condition, and the proportions of: (i) the
634 Fe(III)-reducer *Desulfitobacterium* (25 to 40% of the total sequences) and (ii) the sulphate-
635 reducer *Desulfosporosinus* increased. In the third replicate, Sb was more mobile than in the St
636 condition, the Fe(III)-reducer proportion and identity were different (*Anaeromyxobacter*, “only”
637 3%), and known sulphate-reducers were not detected. Conversely, this replicate exhibited a
638 high proportion of sequences affiliated to the *Bacillus* genus, which includes known Sb(III)-
639 oxidisers (Li et al., 2018) and strains able to grow either in aerobic or anaerobic conditions
640 (Clements et al., 2002). The development of genera including Sb(III)-oxidisers in anoxic
641 conditions seems paradoxical; however, some genera of this metabolic group are facultative

642 anaerobic (*Bacillus*, *Acidithiobacillus*…), thus they could grow in the absence of oxygen, and
643 possibly oxidise Sb(III) using alternative electron acceptors such as nitrate (Terry et al. 2015).
644 Other subtle differences between these replicates could be detected: ORP decreased less
645 sharply, and Fe release was delayed in the microcosm with higher Sb mobility. These results
646 show that Sb behaviour cannot be simply inferred from the redox context and could be strongly
647 influenced by the growth sequence of different microorganisms belonging to different metabolic
648 groups. Divergences of biogeochemical reactions linked with subtle differences in the
649 composition of the initial microbial communities have already been observed in microcosms of
650 sediments (Kwon et al. 2016; Battaglia-Brunet et al. 2022).

651 With the NW, anoxic incubation in the presence of active microbes induced both
652 immobilisation of Sb and a clear increase of the Sb(III) proportion in dissolved Sb (**Table 2**).
653 Immobilisation of Sb in reducing conditions may be linked to Sb(V) reduction, as Sb(III)
654 hydroxide is less soluble than Sb(V) anions in neutral conditions (Brookins 1986; Shkol'nikov
655 2010; Herath et al. 2017), or linked to the precipitation of Sb sulphide in the presence of
656 biogenic H_2S (Zhang et al. 2016). Here, NW AOx incubations induced the growth of bacteria
657 belonging to the *Geobacter* genus, whose proportion of 16S sequences rose from non-
658 detectable in the initial material to 13% on day 20. A *Geobacter* strain (Yamamura et al. 2021)
659 was shown to be able to grow through dissimilatory Sb(V) reduction with acetate as an electron
660 donor, producing Sb_2O_3, and this genus was detected as an active member of an Sb(V)-
661 reducing community in incubated paddy soil (Sun et al. 2021). Hydrogen can be used as an
662 energy source by members of the *Geobacter* genus (Caccavo et al. 1994), and this inorganic
663 substrate was also shown to promote Sb(V) bio-reduction in soils (Nguyen et al. 2018). Thus,
664 *Geobacter*-affiliated organisms could contribute to attenuating Sb mobility in NW incubations.
665 In NAS microcosms incubated in anoxic conditions, Sb mobility was attenuated, and the Sb(V)
666 proportion was slightly lower than in St conditions. In these microcosms, SRB were maintained
667 as a major metabolic group identified at the genus level (2-3%), but the main enriched group
668 corresponded to Fe(III)-reducers, whose proportion increased continuously during incubation,

669 from 4% (day 0) to 8% (day 41). The main Fe(III)-reducers in this group belonged to the genera
670 *Anaeromyxobacter* and *Geothermobacter*. These microcosms contained diverse SRB, and
671 among them, the proportion of *Desulfovibrio*-related sequences slightly increased during
672 incubation. Thus, the biotic stabilisation of Sb in NAS AOx microcosms may have resulted from
673 bio-sulphide precipitation, or bio-reduction of Sb(V) into Sb(III) by some micro-organisms
674 whose Sb(V)-reducing activity has not been yet characterised. These mechanisms could be
675 helped by the generation of Fe(II) by Fe(III)-reducing bacteria, as Fe(II) was shown to
676 accelerate Sb sulphide precipitation by stimulating SRB activity (Xi et al. 2020). In the NAS
677 incubations, dissolved the Fe(II) concentration remained around 2 mg L^{-1}, probably because
678 Fe(II) also precipitated with hydrogen sulphide as FeS. This hypothesis is supported by the
679 darkening of the biotic slurries compared with the St NAS microcosms (Supplementary Fig.
680 8B).

681 Globally, anoxic microbial activities decreased the mobility of Sb; however, they induced a
682 significant release of As in water. The mobilisation of As from mine-contaminated materials in
683 reducing conditions, linked to biological activities, is a well-known phenomenon (Drewniak and
684 Sklodowska 2013; Rajpert et al. 2016), and the antagonist behaviour of Sb and As in mine
685 sediments has previously been described (Casiot et al. 2007).

686

687 **5. Conclusions**

688 Microbial communities inhabiting different surface compartments of a small mining area
689 presented very different compositions. The influence of microbial activities on Sb mobility and
690 speciation was proven in nearly all conditions. Whereas Sb was mainly present in mineral
691 phases resistant to chemical extractions, leaching of soils and sediments released several mg
692 L^{-1} of dissolved Sb. Several microbial activities could contribute to Sb immobilisation, including
693 Fe(II)-oxidation, Sb(V)-reduction, and sulphate-reduction. In aquatic sediments, microbial
694 activities attenuated Sb mobility in both aerobic and anaerobic conditions. Conversely, Sb(III)-

oxidising activities could enhance Sb solubilisation from solid phases of mine wastes. The overall results suggest that microbial processes influencing Sb behaviour on mining sites are very diverse. They should be carefully identified and quantified in each environmental compartment in order to avoid unreliable risk assessments. Moreover, the antagonist biogeochemical behaviour of As and Sb deserves specific awareness as these two toxic elements are very often associated in ore bodies. Specific management options, potentially exploiting microbial reactions, should be developed, aimed to prevent dissemination of these two metalloids in the environment.

Abbreviations: SW, south west; Sb, antimony; As, arsenic; AW, acidic pH waste; NW, neutral pH waste; NAS, neutral pH aquatic sediment; AOx, anoxic conditions; Ox, oxic conditions; St, sterilised; EC, electrical conductivity; ORP, oxidation reduction potential; TOC, total organic carbon.

Acknowledgements

This work was funded by the ANR (ANR-19-MIN2-0002-01), the AEI (MICIU/AEI/REF.: PCI2019-03779) and author's institutions in the framework of the ERA-MIN2 AUREOLE project. J.D.P.P. is the beneficiary of a grant for the requalification of the Spanish university system from the Ministry of Universities of the Government of Spain, financed by the European Union, NextGeneration EU.

Competing interests

The authors declare that they have no known competing financial interests or personal relationships that could have appeared to influence the work reported in this paper.

Author Contributions

The contributions of each author to this study are as follows: Jesus Daniel Peco Palacios to methodology, investigation and writing (original draft preparation, editing); Hugues Thouin to methodology, investigation and writing (original draft preparation, editing); Héctor R. Campos-Rodríguez to investigation and writing (original draft preparation, editing); José María Esbrí to investigation and writing (original draft preparation, editing); Eva Maria García-Noguero, Dominique Breeze and Jaime Villenato to Investigation ; Eric Gloaguen to conceptualisation and resources; Pablo Leon Higueras to conceptualisation, writing (original draft), resources and supervision; Fabienne Battaglia-Brunet to conceptualisation, writing (editing) and supervision.

References

Abin CA, Hollibaugh JT (2017) *Desulfuribacillus stibiiarsenatis* sp. nov. an obligately anaerobic, dissimilatory antimonate- and arsenate-reducing bacterium isolated from anoxic sediments, and emended description of the genus *Desulfuribacillus*. Int J Syst Evol Microbiol 67(4), 1011-1017. https://doi.org/10.1099/ijsem.0.001732.

Alazard D, Joseph M, Battaglia-Brunet F, Cayol JL, Ollivier B (2010) *Desulfosporosinus acidiphilus* sp. nov.: a moderately acidophilic sulfate-reducing bacterium isolated from acid mining drainage sediments. Extremophiles 14, 305–312. https://doi.org/10.1007/s00792-010-0309-4

Anderson CG (2012) The metallurgy of antimony. Geochemistry 72, 3-8. https://doi.or/10.1016/j.chemer.2012.04.001

Andrade CF, Jamieson HE, Kyser TK, Praharaj T, Fortin D (2010) Biogeochemical redox cycling of arsenic in mine-impacted lake sediments and co-existing pore waters near Giant Mine, Yellowknife Bay, Canada. Appl Geochem 25(2), 199-211. https://doi.org/10.1016/j.apgeochem.2009.11.005.

746 Ashley PM, Craw D, Graham BP, Chappell DA (2003) Environmental mobility of antimony
747 around mesothermal stibnite deposits, New South Wales, Australia and southern New
748 Zealand. J Geochem Explor 77, 1-14. https://doi.org/10.1016/S0375-6742(02)00251-0

749 Balk M, Altınbaş M, Rijpstra WIC, Sinninghe D, Jaap S, Stams AJM (2008) *Desulfatirhabdium*
750 *butyrativorans* gen. nov. sp. nov. a butyrate-oxidizing, sulfate-reducing bacterium isolated
751 from an anaerobic bioreactor. Int J Syst Evol Microbiol 58, 110-115.
752 https://doi.org/10.1099/ijs.0.65396-0

753 Battaglia-Brunet F, Naveau A, Cary L, Bueno M, Briais J, Charron M, Joulian C, Thouin H
754 (2022) Biogeochemical behaviour of geogenic As in a confined aquifer of the Sologne
755 region, France. Chemosphere, 304, 135252.
756 https://doi.org/10.1016/j.chemosphere.2022.135252

757 Borcard D, Gillet F, Legendre P (2011) Numerical Ecology with R. Springer, New York, New
758 York, USA.

759 Brookins DG (1986) Geochemical behavior of antimony, arsenic, cadmium and thallium: Eh-
760 pH diagrams for 25°C, 1-bar pressure. Chem Geol 54, Issues 3–4, 271-278.
761 https://doi.org/10.1016/0009-2541(86)90141-5

762 Caccavo F, Lonergan DJ, Lovley DR, Davis M, Stolz JF, Mc Inerney MJ (1994) *Geobacter*
763 *sulfurreducens* sp. nov. a hydrogen- and acetate-oxidizing dissimilatory metal-reducing
764 microorganism. Appl Environ Microbiol 60, 3752-3759.
765 https://doi.org/10.1128/aem.60.10.3752-3759.1994.

766 Caplette JN, Grob M, Mestrot A (2021) Validation and deployment of a quantitative trapping
767 method to measure volatile antimony emissions. Env Pol 289, 117831.
768 https://doi.org/10.1016/j.envpol.2021.117831.

769 Casiot C, Ujevic M, Munoz M, Seidel JL, Elbaz-Poulichet F (2007) Antimony and arsenic
770 mobility in a creek draining an antimony mine abandoned 85 years ago (upper Orb basin,

771 France). Appl Geochemi 22(4), 788-798.
772 https://doi.org/10.1016/j.apgeochem.2006.11.007.

773 Cavaletti L, Monciardini P, Bamonte R, Schumann P, Rohde M, Sosio M, Donadio S (2006)
774 New lineage of filamentous, spore-forming, gram-positive bacteria from soil. Appl Environ
775 Microbiol 72, 4360-4369. https://doi.org/10.1128/AEM.00132-06

776 Cidu R, Biddau R, Dore E (2015) Determination of trace of Sb(III) using ASV in Sb-rich water
777 samples affected by mining. Anal Chim Acta 854, 34–39.
778 https://doi.org/10.1016/j.aca.2014.11.020

779 Cidu R, Dore E, Biddau R, Nordstrom DK (2018) Fate of Antimony and Arsenic in
780 Contaminated Waters at the Abandoned Su Suergiu Mine (Sardinia Italy). Mine Water
781 Environ 37, 151–165. https://doi.org/10.1007/s10230-017-0479-84

782 Clements LD, Miller BS, Streips UN (2002) Comparative Growth Analysis of the Facultative
783 Anaerobes *Bacillus subtilis*, *Bacillus licheniformis*, and *Escherichia coli*. System Appl
784 Microbiol 25, 284-286. https://doi.org/10.1078/0723-2020-00108

785 De Vet WWJM, Dinkla IJT, Rietveld LC, van Loosdrecht MCM (2011) Biological iron oxidation
786 by *Gallionella* spp. in drinking water production under fully aerated conditions. Water Res
787 45(17), 5389-5398. https://doi.org/10.1016/j.watres.2011.07.028

788 Deng D, Weidhaas JL, Lin LS (2016) Kinetics and microbial ecology of batch sulfidogenic
789 bioreactors for co-treatment of municipal wastewater and acid mine drainage. J Hazard
790 Mater 305, 200-208. https://doi.org/10.1016/j.jhazmat.2015.11.041.

791 Deng R, Chen Y, Deng X, Huang Z, Zhou S, Ren B, Jin G, Hursthouse A (2021) A Critical
792 Review of Resistance and Oxidation Mechanisms of Sb-Oxidizing Bacteria for the
793 Bioremediation of Sb(III) Pollution. Front Microbiol 12, 2418.
794 https://doi.org/10.3389/fmicb.2021.738596

795 Deng R, Tang Z, Hou B, et al (2020) Microbial diversity in soils from antimony mining sites:
796 geochemical control promotes species enrichment. Environ Chem Lett 18, 911–922 (2020).
797 https://doi.org/10.1007/s10311-020-00975-1

798 Drewniak L, Sklodowska A (2013) Arsenic-transforming microbes and their role in biomining
799 processes. Environ Sci Pollut Res 20, 7728–7739. https://doi.org/10.1007/s11356-012-
800 1449-0

801 Duan R, Du Y, Chen Z, Zhang Y, Hu W, Yang L, Xiang G, Luo Y (2022) Diversity and
802 composition of soil bacteria between abandoned and selective-farming farmlands in an
803 antimony mining area. Front Microbiol 13:953624.
804 https://doi.org/10.3389/fmicb.2022.953624

805 Dupont D, Arnout S, Jones PT, Binnemans K (2016) Antimony Recovery from End-of-Life
806 Products and Industrial Process Residues: A Critical Review. J Sustain Metall 2, 79–103.
807 https://doi.org.10.1007/s40831-016-0043-y

808 El Shanawany S, Foda N, Hashad DI, Salama N, Sobh Z (2017) The potential DNA toxic
809 changes among workers exposed to antimony trioxide. Environ Sci Pollut Res 24, 12455–
810 12461. https://doi.org.10.1007/s11356-017-8805-z

811 Emerson D, Weiss JV (2004) Bacterial Iron Oxidation in Circumneutral Freshwater Habitats:
812 Findings from the Field and the Laboratory. Geomicrobiol J 21:6, 405-414.
813 https://doi.org.10.1080/01490450490485881

814 Esbrí JM, Minang CM, Rivera S, Madrid-Illescas M, García-Noguero E, González-Valoys A,
815 Maguregui M, Thouin H, Battaglia-Brunet F, Gloaguen E, Higueras PL (2022) Evaluation of
816 antimony availability in a mining context: Impact for the environment, and for mineral
817 exploration and exploitation. Chemosphere 137086.
818 https://doi.org/10.1016/j.chemosphere.2022.137086

819 Escudié F, Auer L, Bernard M, Mariadassou M, Cauquil L, Vidal K et al (2018) FROGS: find,
820 rapidly, OTUs with galaxy solution. Bioinformatics 34(8), 1287-1294.
821 https://doi.org/10.1093/bioinformatics/btx791

822 Fawcett SE, Jamieson HE, Nordstrom DK, McCleskey RB (2015) Arsenic and antimony
823 geochemistry of mine wastes, associated waters and sediments at the Giant Mine,
824 Yellowknife, Northwest Territories, Canada. Appl Geochem 62, 3-17.
825 https://doi.org/10.1016/j.apgeochem.2014.12.012

826 Filella M, Belzile N, Chen YW (2002a) Antimony in the environment: a review focused on
827 natural waters. I Occurrence Earth-Sci Rev 57, 125-176. https://doi.org/10.1016/S0012-
828 8252(01)00070-8

829 Filella M, Philippo S, Belzile N, Chen Y, Quentel F (2009) Natural attenuation processes
830 applying to antimony: A study in the abandoned antimony mine in Goesdorf, Luxembourg.
831 Sci Total Environ 407, 6205-6216. https://doi.org/10.1016/j.scitotenv.2009.08.027

832 Finneran KT, Forbush HM, Gaw VanPraagh CV, Lovley DR (2002) *Desulfitobacterium*
833 *metallireducens* sp. nov. an anaerobic bacterium that couples growth to the reduction of
834 metals and humic acids as well as chlorinated compounds. Int J Syst Evol Microbiol 52(6),
835 1929-1935. https://doi.org/10.1099/00207713-52-6-1929

836 Frohne T, Rinklebe J, Diaz-Bone RA, Du Laing G (2011) Controlled variation of redox
837 conditions in a floodplain soil: Impact on metal mobilization and biomethylation of arsenic
838 and antimony. Geoderma 160(3-4), 414-424.
839 https://doi.org/10.1016/j.geoderma.2010.10.012

840 Gallego S, Esbrí JM, Campos JA, Peco JD, Martin-Laurent F, Higueras P (2021) Microbial
841 diversity and activity assessment in a 100-year-old lead mine. J Hazard 410, 124618.
842 https://doi.org/10.1016/j.jhazmat.2020.124618

843 Gumiel P (1983) Metalogenia de los yacimientos de antimonio de la Península Ibérica.
844 Tecniterrae 54, 120 pp. (in Spanish).

Gumiel P, Arribas A (1987) Antimony deposits in the Iberian Peninsula. Econ Geol 82(6), pp. 1453-1463. https://doi.org/10.2113/gsecongeo.82.6.1453

Hafeez I, Azam M, Amin A, Mahmood Z, Aamir M, Akram A (2017) Microbial Extraction of Antimony from Stibnite of Qillah Abdullah. ASRJETS 28, 117-127.

Hageman PL (2007) Geological survey field leach test for assessing water reactivity and leaching potential of mine wastes soils and other geologic and environmental materials. U.S. Geological Survey Techniques and Methods http://pubs.usgs.gov/tm/2007/05D03/pdf/TM5-D3_508.pdf

Han Y, Zhang F, Wang Q, Zheng S, Guo W, Feng L, Wang G (2016) *Flavihumibacter stibioxidans* sp. nov. an antimony-oxidizing bacterium isolated from antimony mine soil. IJSEM 66, 4676–4680. https://doi.org/10.1099/ijsem.0.001409

He M, Wang N, Long X, Zhang C, Ma C, Zhong Q, Shan J (2019) Antimony speciation in the environment: Recent advances in understanding the biogeochemical processes and ecological effects. J Environ Sci 75, 14-39. https://doi.org/10.1016/j.jes.2018.05.023

Herath I, Vithanage M, Bundschuh J (2017) Antimony as a global dilemma: Geochemistry, mobility, fate and transport. Environ Pollut 223, 545-559. http://dx.doi.org/10.1016/j.envpol.2017.01.057

Hu X, Guo X, He M, Li S (2016) pH-dependent release characteristics of antimony and arsenic from typical antimony-bearing ores. J Environ Sci 44, 171-179. https://doi.org/10.1016/j.jes.2016.01.003

Kaksonen AH, Plumb JJ, Robertson WJ, Franzmann PD, Gibson JAE, Puhakka JA (2004) Culturable Diversity and Community Fatty Acid Profiling of Sulfate-Reducing Fluidized-Bed Reactors Treating Acidic, Metal-Containing Wastewater. Geomicrobiol J 21(7), 469-480. http://dx.doi.org/10.1080/01490450490505455

Kashefi K, Holmes DE, Baross JA, Lovley DE (2003) Thermophily in the Geobacteraceae: *Geothermobacter ehrlichii* gen. nov. sp. nov. a Novel Thermophilic Member of the

871 Geobacteraceae from the “Bag City” Hydrothermal Vent. Appl Environ Microbiol 69, 2985-
872 2993. https://doi.org/10.1128/AEM.69.5.2985-2993.2003

873 Kong L, He M (2016) Mechanisms of Sb (III) photooxidation by the excitation of organic Fe (III)
874 complexes. Environ Sci Technol 50(13), 6974-6982.
875 http://dx.doi.org/10.1021/acs.est.6b00857

876 Krachler M, Emons H, Zheng J (2001) Speciation of antimony for the 21st century: Promises
877 and pitfalls. TrAC Trends Analyt Chem 20, 79–90. https://doi.org/10.1016/S0165-
878 9936(00)00065-0

879 Kwon MJ, O’Loughlin EJ, Boyanov MI, Brulc JM, Johnston ER, Kemner KM, Antonopoulos DA
880 (2016) Impact of Organic Carbon Electron Donors on Microbial Community Development
881 under Iron- and Sulfate-Reducing Conditions. PLOS ONE
882 https://doi.org/10.1371/journal.pone.0146689

883 Leuz AK, Mönch H, Johnson CA (2006) Sorption of Sb(III) and Sb(V) to Goethite: Influence on
884 Sb(III) Oxidation and Mobilization. Environ Sci Technol 40:7277–7282.
885 https://doi.org/10.1021/es061284b

886 Li J, Yu H, Wu X, Shen L, Liu Y, Qiu G, Zeng W, Yu R (2018) Novel Hyper Antimony-Oxidizing
887 Bacteria Isolated from Contaminated Mine Soils in China. Geomicrobiol J 35(8), 713-720.
888 https://doi.org/10.1080/01490451.2018.1454556

889 Loni PC, Wu M, Wang W, Wang H, Ma L, Liu C, Song Y, Tuovinen OH (2020) Mechanism of
890 microbial dissolution and oxidation of antimony in stibnite under ambient conditions. J Haz
891 Mat 385, 121561. https://doi.org/10.1016/j.jhazmat.2019.121561

892 Lotze F (1956) Das Präkambrium Spaniens. N Jb Geol Paläont 8: 373-380.

893 Mamindy-Pajany Y, Bataillard P, Séby F, Crouzet C, Moulin A, Guezennec A-G, Hurel C,
894 Marmier N, Battaglia-Brunet F (2013) Arsenic in marina sediments from the Mediterranean
895 coast: speciation in the solid phase and occurrence of thioarsenates. Soil Sediment
896 Contam 22, 984–1002. https://doi.org/10.1080/15320383.2013.770441

897 Mitsunobu S, Harada T, Takahashi Y (2006) Comparison of antimony behavior with that of
898 arsenic under various soil redox conditions. Environ Sci Technol 40(23), 7270-7276.
899 https://doi.org/10.1007/BF02839926

900 Molecular Probes (2004) LIVE/DEAD BacLight Bacterial Viability Kit product information.
901 Handbook of fluorescent probes and research products.

902 Murti GK, Volk V, Jackson M (1966) Colorimetric determination of iron of mixed valency by
903 orthophenanthroline. Soil Sci Soc Am J 30, 663–664.
904 https://doi.org/10.2136/sssaj1966.03615995003000050037x

905 Nguyen VK, Choi W, Park Y, Yu J, Lee T (2018) Characterization of diversified Sb(V)-reducing
906 bacterial communities by various organic or inorganic electron donors. Bioresour Technol
907 250, 239-246. https://doi.org/10.1016/j.biortech.2017.11.044.

908 Nguyen VK, Lee JU (2014) Isolation and Characterization of Antimony-Reducing Bacteria from
909 Sediments Collected in the Vicinity of an Antimony Factory. Geomicrobiol J 31(10), 855-
910 861. https://doi.org/10.1080/01490451.2014.901440.

911 Nguyen VK, Lee JU (2015) Antimony-Oxidizing Bacteria Isolated from Antimony-Contaminated
912 Sediment – A Phylogenetic Study, Geomicrobiol J 32(1), 50-58.
913 https://doi.org/10.1080/01490451.2014.925009

914 Otte JM, Blackwell N, Soos V, Rughöft S, Maisch M, Kappler A, Kleindienst S, Schmidt C
915 (2018) Sterilization impacts on marine sediment-Are we able to inactivate microorganisms
916 in environmental samples? FEMS Microbiol Ecol 94(12) December 2018, fiy189.
917 https://doi.org/10.1093/femsec/fiy189

918 Pitman AL, Pourbaix M, de Zoubov N (1957) Potential-pH Diagram of the Antimony-Water
919 System: Its Applications to Properties of the Metal, Its Compounds, Its Corrosion, and
920 Antimony Electrodes. J Electrochem Soc 104, 594-600. https://doi.org/10.1149/1.2428423

921 Polack R, Chen YW, Belzile N (2009) Behaviour of Sb(V) in the presence of dissolved sulfide
922 under controlled anoxic aqueous conditions. Chem Geol 262, 179-185.
923 https://doi.org/10.1016/j.chemgeo.2009.01.008.

924 Quatrini R, Johnson DB (2019) *Acidithiobacillus ferrooxidans*. Trends Microbiol.
925 https://doi.org/10.1016/j.tim.2018.11.009

926 Quevauviller P, Rauret G, López-Sánchez J, Rubio R, Ure A, Muntau H (1997) Certification of
927 trace metal extractable contents in a sediment reference material (CRM 601) following a
928 three-step sequential extraction procedure. Sci Total Environ 205(2-3), 223-234.
929 https://doi.org/10.1016/S0048-9697(97)00205-2

930 Radková AB, Jamieson HE, Campbell KM (2020) Antimony mobility during the early stages of
931 stibnite weathering in tailings at the Beaver Brook Sb deposit, Newfoundland. Appl
932 Geochem 115, 104528. https://doi.org/10.1016/j.apgeochem.2020.104528

933 Rajpert L, Kolvenbach BA, Ammann EM, Hockmann K, Nachtegaal M, Eichel E, Schäffer A,
934 Corvini PFX, Skłodowska A, Lenz M (2016) Arsenic Mobilization from Historically
935 Contaminated Mining Soils in a Continuously Operated Bioreactor: Implications for Risk
936 Assessment. Environ Sci Technol 50(17), 9124–9132.
937 https://doi.org/10.1021/acs.est.6b02037

938 Roper AJ, Williams PA, Filella M (2012) Secondary antimony minerals: Phases that control the
939 dispersion of antimony in the supergene zone. Geochemistry 72, 9-14.
940 https://doi.org/10.1016/j.chemer.2012.01.005

941 Sánchez-Andrea I, Knittel K, Amann R, Amils R, Sanz JL (2012) Quantification of Tinto River
942 Sediment Microbial Communities: Importance of Sulfate-Reducing Bacteria and Their Role
943 in Attenuating Acid Mine Drainage. Appl Environ Microbiol 78, 4638-4645.
944 https://doi.org/10.1128/AEM.00848-12

945 Schildroth S, Osborne G, Smith AR, Yip C, Collins C, Smith MT, Sandy MS, Zhang L (2021)
946 Occupational exposure to antimony trioxide: a risk assessment. Occup Environ Med 78,
947 413-418. https://oem.bmj.com/content/78/6/413.full.pdf

948 Schnitzer M (1983) Organic matter characterization. Methods of Soil Analysis: Part 2.
949 Chemical and Microbiological Properties 9, 581-594.
950 https://doi.org/10.2134/agronmonogr9.2.2ed.c30

951 Shkol'nikov EV (2010) Thermodynamic characterization of the amphoterism of oxides M_2O_3
952 (M = As, Sb, Bi) and Their hydrates in aqueous media. Russ J Appl Chem 83, 2121–2127.
953 https://doi.org/10.1134/S1070427210120104

954 Sun L-N, Guo B, Lyu W-G, Tang X-J (2020) Genomic and physiological characterization of an
955 antimony and arsenite-oxidizing bacterium *Roseomonas rhizosphaerae*. Env Res 191,
956 110136. https://doi.org/10.1016/j.envres.2020.110136

957 Sun W, Sun X, Häggblom MM, Kolton M, Lan L, Li B, Dong Y, Xu R, Li F (2021) Identification
958 of Antimonate Reducing Bacteria and Their Potential Metabolic Traits by the Combination
959 of Stable Isotope Probing and Metagenomic-Pangenomic. Analysis Environ Sci Technol 55,
960 20, 13902–13912. https://doi.org/10.1021/acs.est.1c03967

961 Sun W, Xiao E, Dong Y, Tang S, Krumins V, Ning Z, Sun M, Zhao Y, Wu S, Xiao T (2016)
962 Profiling microbial community in a watershed heavily contaminated by an active antimony
963 (Sb) mine in Southwest China. Sci Total Environ 550, 297-308.
964 https://doi.org/10.1016/j.scitotenv.2016.01.090.

965 Sundar S, Chakravarty J (2010) Antimony Toxicity. Int J Environ Res Public Health 7, 4267-
966 4277. https://doi.org/10.3390/ijerph7124267

967 Terry LR, Kulp TR, Wiatrowski H, Miller LG, Oremland RS (2015) Microbiological Oxidation of
968 Antimony(III) with Oxygen or Nitrate by Bacteria Isolated from Contaminated Mine
969 Sediments. Appl Environ Microbiol 81, 8478-8488. https://doi.org/10.1128/AEM.01970-15

970 Torma AE, Gabra GG (1977) Oxidation of stibnite by *Thiobacillus ferrooxidans*. Antonie van
971 Leeuwenhoek 43, 1-6. https://doi.org/10.1007/BF02316204

972 Treude N, Rosencrantz D, Liesack W, Schnell S (2003) Strain FAc12, a dissimilatory iron-
973 reducing member of the Anaeromyxobacter subgroup of Myxococcales, FEMS Microbiol
974 Ecol 44(2), 261–269. https://doi.org/10.1016/S0168-6496(03)00048-5

975 USGS (2021) Mineral Commodity Summaries, January
976 https://pubs.usgs.gov/periodicals/mcs2021/mcs2021-antimony.pdf

977 Wang X, Yang Y, Tao L, He M (2021) Antimonite oxidation and adsorption onto two tunnel-
978 structured manganese oxides: Implications for antimony mobility. Chem Geol 579, 120336.
979 https://doi.org/10.1016/j.chemgeo.2021.120336

980 Wang Z, Tollervey J, Briese M, et al (2009) CLIP: Construction of cDNA libraries for high-
981 throughput sequencing from RNAs cross-linked to proteins in vivo. Methods 48, 287–293.
982 https://doi.org/10.1016/j.ymeth.2009.02.021

983 Weiss JV, Rentz JA, Plaia T, Neubauer SC, Merrill-Floyd MT, Lilburn Bradburne C, Megonigal
984 JP, Emerson D (2007) Characterization of Neutrophilic Fe(II)-Oxidizing Bacteria Isolated
985 from the Rhizosphere of Wetland Plants and Description of Ferritrophicum radicicola gen.
986 nov. sp. nov. and *Sideroxydans paludicola* sp. nov. Geomicrobiol J 24(7-8), 559-570.
987 https://doi.org/10.1080/01490450701670152

988 Wen B, Zhou J, Zhou A, Liu C, Xie L (2016) Sources, migration and transformation of antimony
989 contamination in the water environment of Xikuangshan, China: Evidence from geochemical
990 and stable isotope (S, Sr) signatures. Sci Total Environ 569–570, 114-122.
991 https://doi.org/10.1016/j.scitotenv.2016.05.124

992 Wilson SC, Lockwood PV, Ashley PM, Tighe M (2010) The chemistry and behaviour of
993 antimony in the soil environment with comparisons to arsenic: a critical review. Environ
994 Pollut 158(5), 1169-1181. https://doi.org/10.1016/j.envpol.2009.10.045

995 Xi YS, Lan S, Li X, Wu Y, Yuan X, Zhang C, Yunguo L, Huang Y, Quan B, Wu S (2020)
996 Bioremediation of antimony from wastewater by sulfate-reducing bacteria: Effect of the
997 coexisting ferrous ion. I Biodeterior Biodegradation 148, 104912.
998 https://doi.org/10.1016/j.ibiod.2020.104912

999 Xiang L, Liu C, Liu D, Ma L, Qiu X, Wang H, Lu X (2022) Antimony transformation and
1000 mobilization from stibnite by an antimonite oxidizing bacterium Bosea sp. AS-1. J. Environ.
1001 Sci 111, 273-281. https://doi.org/10.1016/j.jes.2021.03.042

1002 Yamamura S, Iida C, Kobayashi Y, Watanabe M, Amachi S (2021) Production of two
1003 morphologically different antimony trioxides by a novel antimonate-reducing bacterium,
1004 *Geobacter* sp. SVR. J Hazard Mater 411, 125100.
1005 https://doi.org/10.1016/j.jhazmat.2021.125100

1006 Yang H, Gao K, Feng S, Zhang L, Wang W (2015) Isolation of sulfide remover strain
1007 *Thermithiobacillus tepidarius* JNU-2, and scale-up bioreaction for sulfur regeneration. Ann
1008 Microbiol 65, 553–563. https://doi.org/10.1007/s13213-014-0891-2

1009 Yang Z, Hosokawa H, Sadakane T, Kuroda M, Inoue D, Nishikawa H, Ike M (2020) Isolation
1010 and Characterization of Facultative-Anaerobic Antimonate-Reducing Bacteria.
1011 Microorganisms 8, 1435. https://doi.org/10.3390/microorganisms8091435

1012 Ye L, Chen H, Jing C (2019) Sulfate-Reducing Bacteria Mobilize Adsorbed Antimonate by
1013 Thioantimonate Formation. Environ Sci Technol Lett 6, 418–422.
1014 https://doi.org/10.1021/acs.estlett.9b00353.

1015 Yu C, Cai Q, Guo ZX, Yang Z, Khoo SB (2002) Antimony speciation by inductively coupled
1016 plasma mass spectrometry using solid phase extraction cartridges. Analyst 127, 380-1385.
1017 https://doi.org/10.1039/B206829J

1018 Zhang G, Ouyang X, Li H, Fu Z, Chen J (2016) Bioremoval of antimony from contaminated
1019 waters by a mixed batch culture of sulfate-reducing bacteria. Int Biodeter Biodegradation
1020 115, 148-155. https://doi.org/10.1016/j.ibiod.2016.08.007